



MIT Open Access Articles

Search for a massive resonance decaying to a pair of Higgs bosons in the four b quark final state in proton–proton collisions at $\sqrt{s} = 13$ TeV

The MIT Faculty has made this article openly available. **Please share** how this access benefits you. Your story matters.

Citation	Sirunyan, A. M., et al. "Search for a Massive Resonance Decaying to a Pair of Higgs Bosons in the Four b Quark Final State in Proton–Proton Collisions at $\sqrt{s} = 13$ TeV." <i>Physics Letters B</i> , vol. 781, June 2018, pp. 244–69. © 2018 The Authors
As Published	http://dx.doi.org/10.1016/J.PHYSLETB.2018.03.084
Publisher	Elsevier BV
Version	Final published version
Citable link	http://hdl.handle.net/1721.1/119365
Terms of Use	Creative Commons Attribution 4.0 International License
Detailed Terms	http://creativecommons.org/licenses/by/4.0/



Search for a massive resonance decaying to a pair of Higgs bosons in the four b quark final state in proton–proton collisions at $\sqrt{s} = 13$ TeV

The CMS Collaboration ^{*}

CERN, Switzerland



ARTICLE INFO

Article history:

Received 13 October 2017
 Received in revised form 23 March 2018
 Accepted 29 March 2018
 Available online 4 April 2018
 Editor: M. Doser

Keywords:

CMS
 Physics
 Extradimensions
 Graviton
 Radion
 di-Higgs boson resonance

ABSTRACT

A search for a massive resonance decaying into a pair of standard model Higgs bosons, in a final state consisting of two b quark–antiquark pairs, is performed. A data sample of proton–proton collisions at a centre-of-mass energy of 13 TeV is used, collected by the CMS experiment at the CERN LHC in 2016, and corresponding to an integrated luminosity of 35.9 fb^{-1} . The Higgs bosons are highly Lorentz-boosted and are each reconstructed as a single large-area jet. The signal is characterized by a peak in the dijet invariant mass distribution, above a background from the standard model multijet production. The observations are consistent with the background expectations, and are interpreted as upper limits on the products of the s-channel production cross sections and branching fractions of narrow bulk gravitons and radions in warped extra-dimensional models. The limits range from 126 to 1.4 fb at 95% confidence level for resonances with masses between 750 and 3000 GeV, and are the most stringent to date, over the explored mass range.

© 2018 The Author(s). Published by Elsevier B.V. This is an open access article under the CC BY license (<http://creativecommons.org/licenses/by/4.0/>). Funded by SCOAP³.

1. Introduction

In the standard model (SM), the pair production of Higgs bosons (H) [1–3] in proton–proton (pp) collisions at $\sqrt{s} = 13$ TeV is a rare process [4]. However, the existence of massive resonances decaying to Higgs boson pairs (HH) in many new physics models may enhance this rate to a level observable at the CERN LHC using the current data. For instance, models with warped extra dimensions (WED) [5] contain new particles such as the spin-0 radion [6–8] and the spin-2 first Kaluza–Klein (KK) excitation of the graviton [9–11], which have sizeable branching fractions to HH.

The WED models have an extra spatial dimension compactified between two branes, with the region between (called the bulk) warped via an exponential metric κl , κ being the warp factor and l the coordinate of the extra spatial dimension [12]. The reduced Planck scale ($\overline{M}_{\text{Pl}} \equiv M_{\text{Pl}}/8\pi$, M_{Pl} being the Planck scale) is considered a fundamental scale. The free parameters of the model are $\kappa/\overline{M}_{\text{Pl}}$ and the ultraviolet cutoff of the theory $\Lambda_{\text{R}} \equiv \sqrt{6}e^{-\kappa l}\overline{M}_{\text{Pl}}$ [6]. In pp collisions at the LHC, the graviton and the radion are produced primarily through gluon–gluon fusion and are predicted to decay to HH [13].

Other scenarios, such as the two-Higgs doublet models [14] (in particular, the minimal supersymmetric model [15]) and the

Georgi–Machacek model [16] predict spin-0 resonances that are produced primarily through gluon–gluon fusion, and decay to an HH pair. These particles have the same Lorentz structure and effective couplings to the gluons and, for narrow widths, result in the same kinematic distributions as those for the bulk radion. Hence, the results of this paper are also applicable to this class of models.

Searches for a new particle X in the HH decay channel have been performed by the ATLAS [17–19] and CMS [20–24] Collaborations in pp collisions at $\sqrt{s} = 7$ and 8 TeV. More recently, the ATLAS Collaboration has published limits on the production of a KK bulk graviton, decaying to HH, in the $\overline{b\overline{b}b\overline{b}}$ final state, using pp collision data at $\sqrt{s} = 13$ TeV, corresponding to an integrated luminosity of 3.2 fb^{-1} [25]. Because the longitudinal components of the W and Z bosons couple to the Higgs field in the SM, a resonance decaying to HH potentially also decays into WW and ZZ, with a comparable branching fraction for $X \rightarrow ZZ$, and with a branching fraction for $X \rightarrow WW$ that is twice as large. Searches for $X \rightarrow WW$ and ZZ have been performed by ATLAS and CMS [26–35].

This letter reports on the search for a massive resonance decaying to an HH pair, in the $\overline{b\overline{b}b\overline{b}}$ final state (with a branching fraction $\approx 33\%$ [36]), performed using a data set corresponding to 35.9 fb^{-1} of pp collisions at $\sqrt{s} = 13$ TeV. The search significantly improves upon the CMS analysis performed using the LHC data collected at $\sqrt{s} = 8$ TeV [24], and extends the searched mass range to 750–3000 GeV. This search is conducted for both the radion

^{*} E-mail address: cms-publication-committee-chair@cern.ch.

and the graviton, whereas the earlier search only considered the former.

In this search, the $X \rightarrow HH$ decay would result in highly Lorentz-boosted and collimated decay products of $H \rightarrow b\bar{b}$, which are referred to as H jets. These are reconstructed using jet substructure and jet flavour-tagging techniques [37–39]. The background consists mostly of SM multijet events, and is estimated using several control regions defined in the phase space of the masses and flavour-tagging discriminators of the two H jets, and the HH dijet invariant mass, allowing the background to be predicted over the entire range of m_X explored. The signal would appear as a peak in the HH dijet invariant mass spectrum above a smooth background distribution.

2. The CMS detector and event simulations

The CMS detector with its coordinate system and the relevant kinematic variables is described in Ref. [40]. The central feature of the CMS apparatus is a superconducting solenoid of 6 m internal diameter, providing a magnetic field of 3.8 T. Within the field volume are silicon pixel and strip trackers, a lead tungstate crystal electromagnetic calorimeter (ECAL), and a brass and scintillator hadron calorimeter (HCAL), each composed of a barrel and two endcap sections. The tracker covers a pseudorapidity η range from -2.5 to 2.5 with the ECAL and the HCAL extending up to $|\eta| = 3$. Forward calorimeters in the region up to $|\eta| = 5$ provide almost hermetic detector coverage. Muons are detected in gas-ionization chambers embedded in the steel flux-return yoke outside the solenoid, covering a region of $|\eta| < 2.4$.

Events of interest are selected using a two-tiered trigger system [41]. The first level (L1), composed of custom hardware processors, uses information from the calorimeters and muon detectors to select events at a rate of around 100 kHz. The second level, known as the high-level trigger (HLT), consists of a farm of processors running a version of the full event reconstruction software optimized for fast processing, and reduces the event rate to around 1 kHz before data storage. Events are selected at the trigger level by the presence of jets of particles in the detector. The L1 trigger algorithms reconstruct jets from energy deposits in the calorimeters. At the HLT, physics objects (charged and neutral hadrons, electrons, muons, and photons) are reconstructed using a particle-flow (PF) algorithm [42]. The anti- k_T algorithm [43,44] is used to cluster these objects with a distance parameter of 0.8 (AK8 jets) or 0.4 (AK4 jets).

Bulk graviton and radion signal events are simulated at leading order using the MADGRAPH5_AMC@NLO 2.3.3 [45] event generator for masses in the range 750–3000 GeV and widths of 1 MeV (narrow width approximation). The NNPDF3.0 leading order parton distribution functions (PDFs) [46], taken from the LHAPDF6 PDF set [47–50], with the four-flavour scheme, is used. The showering and hadronization of partons is simulated with PYTHIA 8.212 [51]. The HERWIG++ 2.7.1 [52] generator is used for an alternative model to evaluate the systematic uncertainty associated with the parton shower and hadronization. The tune CUETP8M1-NNPDF2.3LO [53] is used for PYTHIA 8, while the EE5C tune [54] is used for HERWIG++.

The background is modelled entirely from data. However, simulated background samples are used to develop and validate the background estimation techniques, prior to being applied to the data. These are multijet events, generated at leading order using MADGRAPH5_AMC@NLO, and $t\bar{t}$ + jets, generated at next-to-leading order using POWHEG 2.0 [55–57]. Both these backgrounds are interfaced to PYTHIA 8 for simulating the parton shower and hadronization. Studies using simulations established that the multijet com-

ponent is more than 99% of the background, with the rest mostly from $t\bar{t}$ + jets production.

All generated samples were processed through a GEANT4-based [58,59] simulation of the CMS detector. Multiple pp collisions may occur in the same or adjacent LHC bunch crossings (pileup) and contribute to the overall event activity in the detector. This effect is included in the simulations, and the samples are reweighted to match the number of pp interactions observed in the data, assuming a total inelastic pp collision cross section of 69.2 mb [60].

3. Event selection

Events were collected using several HLT algorithms. The first required the scalar p_T sum of all AK4 jets in the event (H_T) to be greater than 800 or 900 GeV, depending on the LHC beam instantaneous luminosity. A second trigger criterion required $H_T \geq 650$ GeV, with a pair of AK4 jets with invariant mass above 900 GeV and a pseudorapidity separation $|\Delta\eta| < 1.5$. A third set of triggers selected events with the scalar p_T sum of all AK8 jets greater than 650 or 700 GeV and the presence of an AK8 jet with a “trimmed mass” above 50 GeV, i.e. the jet mass after removing remnants of soft radiation using jet trimming technique [61]. The fourth triggering condition was based on the presence of an AK8 jet with $p_T > 360$ GeV and trimmed mass greater than 30 GeV. The last trigger selection accepted events containing two AK8 jets having $p_T > 280$ and 200 GeV with at least one having trimmed mass greater than 30 GeV, together with an AK4 jet passing a loose b-tagging criterion.

The pp interaction vertex with the highest $\sum p_T^2$ of the associated clusters of physics objects is considered to be the one associated with the hard scattering interaction, the primary vertex. The physics objects are the jets, clustered using the jet finding algorithm [43,44] with the tracks assigned to the vertex as inputs, and the associated missing transverse momentum, taken as the negative vector sum of the p_T of those jets. The other interaction vertices are designated as pileup vertices.

To mitigate the effect of pileup, particles are assigned weights using the pileup per particle identification (PUPPI) algorithm [62], with the weight corresponding to its estimated probability to originate from a pileup interaction. Charged particles from pileup vertices receive a weight of zero while those from the primary vertex receive a weight of one. Neutral particles are assigned a weight between zero and one, with higher values for those likely to originate from the primary vertex. Particles are then clustered into AK8 jets. The vector sum of the weighted momenta of all particles clustered in the jet is taken to be the jet momentum. To account for detector response nonlinearity, jet energy corrections are applied as a function of jet η and p_T [63,64]. In each event, the leading and the subleading p_T AK8 jets, j_1 and j_2 , respectively, are required to have $p_T > 300$ GeV and $|\eta| < 2.4$.

The removal of events containing isolated leptons (electrons or muons) with $p_T > 20$ GeV and $|\eta| < 2.4$ helps suppress $t\bar{t}$ + jets and diboson backgrounds. The isolation variable is defined as the scalar p_T sum of the charged and neutral hadrons, and photons in a cone of $\Delta R = 0.3$ for an electron or $\Delta R = 0.4$ for a muon, where $\Delta R \equiv \sqrt{(\Delta\eta)^2 + (\Delta\phi)^2}$, ϕ being the azimuthal angle in radians. The energy from pileup deposited in the isolation cone, and the p_T of the lepton itself, is subtracted [65,66]. The isolation requirement removes jets misidentified as leptons. Additional quality criteria are applied to improve the purity of the isolated lepton samples. Electrons passing combined isolation and quality criteria corresponding to a selection efficiency of 90% (70%) are designated “loose” (“medium”) electrons. For the “loose” (“medium”) muons, the total associated efficiency is 100% (95%). The probability of a jet to be misidentified as an electron or a muon is in the range

0.5–2%, depending on p_T , η , and the choice of medium or loose selection criteria. Events containing one medium lepton, or two loose leptons of the same flavour, but of opposite charge, are rejected.

The $H \rightarrow b\bar{b}$ system is reconstructed as a single high- p_T AK8 jet, where the decay products have merged within the jet, and the two highest p_T jets in the event are assumed to be the Higgs boson candidates. The jet is groomed [67] to remove soft and wide-angle radiation using the soft-drop algorithm [68,69], with the soft radiation fraction parameter z set to 0.1 and the angular exponent parameter β set to 0. The groomed jet is used to compute the soft-drop jet mass, which peaks at the Higgs boson mass for signal events and reduces the mass of background quark- and gluon-initiated jets. Dedicated mass corrections [70], derived from simulation and data in a region enriched with $t\bar{t}$ events with merged $W \rightarrow q\bar{q}$ decays, are applied to the jet mass in order to remove residual dependence on the jet p_T , and to match the jet mass scale and resolution observed in data.

The soft-drop masses of j_1 and j_2 are required to be within the range 105–135 GeV, with an efficiency of about 60–70%, for jets arising from a signal of mass m_X in the range 750–3000 GeV. The “N-subjettiness” algorithm is used to determine the consistency of the jet with two subjets from a two-pronged $H \rightarrow b\bar{b}$ decay, by computing the inclusive jet shape variables τ_1 and τ_2 [71]. The ratio $\tau_{21} \equiv \tau_2/\tau_1$ with a value much less than one indicates a jet with two subjets. The selection $\tau_{21} < 0.55$ is used, having a jet p_T -dependent efficiency of 50–70%, before applying the soft-drop mass requirement.

For background events, j_1 and j_2 are often well separated in η , especially at high invariant mass (m_{jj}) of j_1 and j_2 . In contrast, signal events that contain a heavy resonance decaying to two energetic H jets are characterized by a small separation of the two jets in η . Events are therefore required to have a pseudorapidity separation $|\Delta\eta(j_1, j_2)| < 1.3$.

The efficiency of the trigger combination is measured in a sample of multijet events, collected with a control trigger requiring a single AK4 jet with $p_T > 260$ GeV, and with the leading and the subleading p_T AK8 jets, j_1 and j_2 , respectively, passing the above selections on p_T , η , and the soft-drop mass. The efficiency is greater than 99% for $m_{jj} \geq 1100$ GeV, and in the range 40–99% for $750 < m_{jj} < 1100$ GeV. The trigger efficiency of the simulated samples is corrected using a scale factor to match the observed efficiency in the data. This scale factor is applied as a function of $|\Delta\eta(j_1, j_2)|$ because it has a mild dependence on this variable.

The main method to suppress the multijet background is b tagging: since a true $H \rightarrow b\bar{b}$ jet contains two b hadrons, the H jet candidates are identified using the dedicated “double-b tagger” algorithm [72]. The double-b tagger exploits the presence of two hadronized b quarks inside the H jet, and uses variables related to b hadron lifetime and mass to distinguish between H jets and the background from multijet production; it also exploits the fact that the b hadron flight directions are strongly correlated with the axes used to calculate the N-subjettiness observables. The double-b tagger is a multivariate discriminator with output between -1 and 1 , with a higher value indicating a greater probability for the jet to contain a $b\bar{b}$ pair. The double-b tagger discriminator thresholds of 0.3 and 0.8 correspond to H jet tagging efficiencies of 80 and 30% and are referred to as “loose” (L) and “tight” (T) requirements, respectively. Events must have the two leading p_T AK8 jets satisfying the loose double-b tagger requirement. The data-to-simulation scale factor for the double-b tagger efficiency is measured in an event sample enriched in $b\bar{b}$ pairs from gluon splitting [72], and applied to the signals to obtain the correct signal yields.

The main variable used in the search for a HH resonance is the “reduced dijet invariant mass” $m_{jj,\text{red}} \equiv m_{jj} - (m_{j_1} - m_H) -$

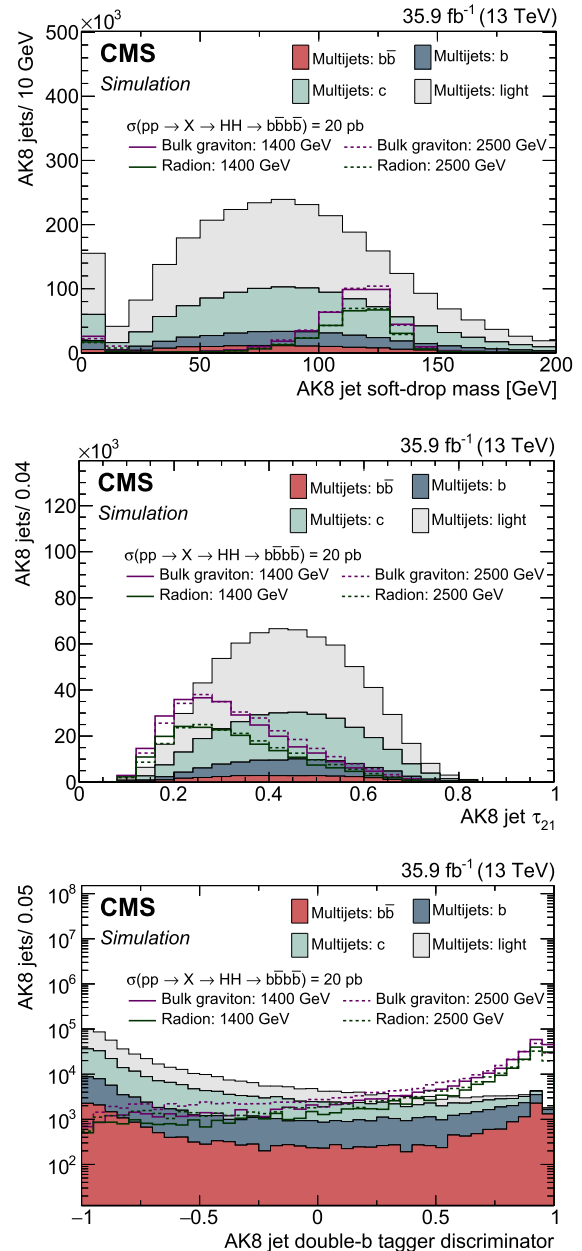


Fig. 1. The soft-drop mass (upper), the N-subjettiness τ_{21} (middle), and the double-b tagger discriminator (lower) distributions of the selected AK8 jets. The multijet background components for the different jet flavours are shown: jets having two B hadrons ($b\bar{b}$) or a single one (b), jets having a charm hadron (c), and all other jets (light). Also plotted are the distributions for the simulated bulk graviton and radion signals of masses 1400 and 2500 GeV. The number of signal and background events correspond to an integrated luminosity of 35.9 fb^{-1} . A signal cross section $\sigma(pp \rightarrow X \rightarrow HH \rightarrow b\bar{b}b\bar{b}) = 20 \text{ pb}$ is assumed for all the mass hypotheses. The events are required to have passed the trigger selection, lepton rejection, the AK8 jet kinematic selections $p_T > 300$ GeV and $|\eta| < 2.4$, and $|\Delta\eta(j_1, j_2)| < 1.3$. The reduced dijet invariant mass $m_{jj,\text{red}}$ is required to be greater than 750 GeV. The N-subjettiness requirement of $\tau_{21} < 0.55$ is applied to the upper and lower figures. The soft-drop masses of the two jets are between 105–135 GeV for the middle and lower figures.

$(m_{j_2} - m_H)$, where m_{j_1} and m_{j_2} are the soft-drop masses of the leading and subleading H-tagged jets in the event, and $m_H = 125.09 \text{ GeV}$ [73,74] is the Higgs boson mass. The quantity $m_{jj,\text{red}}$ is used rather than m_{jj} since by subtracting the soft-drop masses of the two H-tagged jets and adding back the exact Higgs boson mass m_H , fluctuations in m_{j_1} and m_{j_2} due to the jet mass resolu-

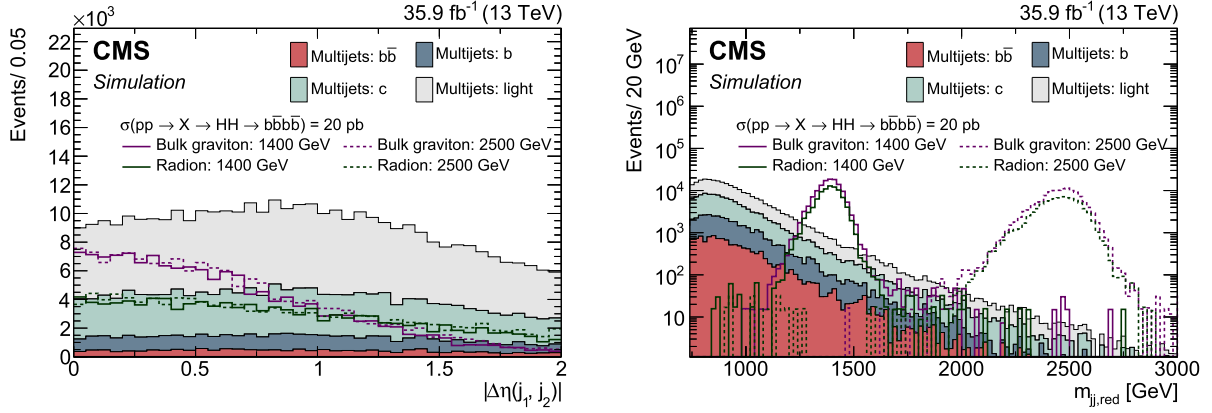


Fig. 2. The jet separation $|\Delta\eta(j_1, j_2)|$ (left) and the reduced dijet invariant mass $m_{jj,red}$ (right) distributions. The multijet background components for the different jet flavours are shown: events containing at least one jet with two B hadrons ($b\bar{b}$) or a single one (b), events containing a jet having a charm hadron (c), and all other events (light). Also plotted are the distributions for the simulated bulk graviton and radion signals of masses 1400 and 2500 GeV. The numbers of signal and background events correspond to an integrated luminosity of 35.9 fb^{-1} . The signal cross section $\sigma(pp \rightarrow X \rightarrow HH \rightarrow b\bar{b}b\bar{b}) = 20 \text{ pb}$ is assumed to be 20 pb for all the mass hypotheses. The events are required to have passed the online selection, lepton rejection, the AK8 jet kinematic selections $p_T > 300 \text{ GeV}$, $|\eta| < 2.4$. The soft-drop masses of the two jets are between 105 and 135 GeV, and the N-subjettiness requirement of $\tau_{21} < 0.55$ and $m_{jj,red} > 750 \text{ GeV}$ are applied. The $m_{jj,red}$ distributions (right) require $|\Delta\eta(j_1, j_2)| < 1.3$.

tion are corrected, leading to 8–10% improvement in the dijet mass resolution. A requirement of $m_{jj,red} > 750 \text{ GeV}$ is applied for selecting signal-like events.

The soft-drop mass, τ_{21} , and double-b tagger discriminator distributions of the two leading p_T jets are shown in Fig. 1 for simulated events after passing the online selection, lepton rejection, kinematic selection, and the requirement $m_{jj,red} > 750 \text{ GeV}$. Also, the N-subjettiness requirement of $\tau_{21} < 0.55$ is applied for the soft-drop mass and the double-b tagger distributions, while the soft-drop mass requirement is applied to the τ_{21} , and double-b tagger discriminator distributions. Since some of the triggers impose a trimmed jet mass requirement, this affects the shape of the offline soft-drop jet mass, resulting in a steep rise above $\sim 20 \text{ GeV}$. The distributions of the $|\Delta\eta(j_1, j_2)|$ and the $m_{jj,red}$ variables are shown in Fig. 2. In these figures, the multijet background is shown for different jet flavour categories: jets having two B hadrons ($b\bar{b}$) or a single one (b), jets having a charm hadron (c), and all other jets (light).

The double-b tagger discriminator of the two leading AK8 jets must exceed the loose threshold. In addition, if both discriminator values also exceed the tight threshold, events are classified in the “TT” category. Otherwise, they are classified in the “LL” category, which contains events with both j_1 and j_2 failing the tight threshold as well as events with either j_1 or j_2 passing the tight threshold while the other passes the loose threshold only.

The backgrounds are estimated separately for each category, and the combination of the likelihoods for the TT and LL categories gives the optimal signal sensitivity over a wide range of resonance masses, according to studies performed using simulated signal and multijet samples. The TT category has a good background rejection for m_X up to 2000 GeV. At higher resonance masses, where the background is small, the LL category provides better signal sensitivity. The full event selection efficiencies for bulk gravitons and radions of different assumed masses are shown in Fig. 3. The radion has a smaller efficiency than the bulk graviton because its $|\Delta\eta(j_1, j_2)|$ distribution is considerably wider than that of a bulk graviton of the same mass, as shown in Fig. 2 (left).

4. Signal and background modelling

The method chosen for the background modelling depends on whether the resonance mass m_X is below or above 1200 GeV, since at low masses the background does not fall smoothly as a func-

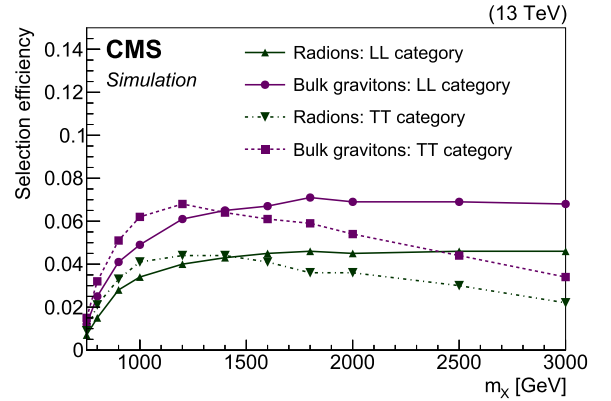


Fig. 3. The signal selection efficiencies for the bulk graviton and radion models for different mass hypotheses of the resonances, shown for the LL and the TT signal event categories. Owing to the large sample sizes of the simulated events, the statistical uncertainties are small.

tion of $m_{jj,red}$, because of the trigger requirements, while above 1200 GeV it does. The background estimation relies on a set of control regions to predict the total background shape and normalization in the signal regions. The entire range of the $m_{jj,red}$ distribution above 750 GeV is used for the prediction.

For signals with $m_X \geq 1200 \text{ GeV}$, the underlying background distribution falls monotonically with $m_{jj,red}$, thus allowing the background shape to be modelled by a smooth function, above which a localized signal is searched for. This smooth background modelling helps to reduce uncertainties in the background estimation from local statistical fluctuations in $m_{jj,red}$, thereby improving the signal search sensitivity. The parameters of the function and its total normalization are constrained by a simultaneous fit of the signal and background models to the data in the control and the signal regions. For $m_X \geq 1200 \text{ GeV}$, the $m_{jj,red}$ distributions for the signal are modelled using the sum of a Gaussian and a Crystal Ball function [75], as shown in Fig. 4 for one signal category. The same modelling is used for the other signal categories, with different parameters for the Gaussian and the Crystal Ball functions.

The signal and control regions are defined by two variables related to the leading p_T jet j_1 : (i) its soft-drop mass m_{j_1} and (ii) the value of the discriminator of the double-b tagger. The background

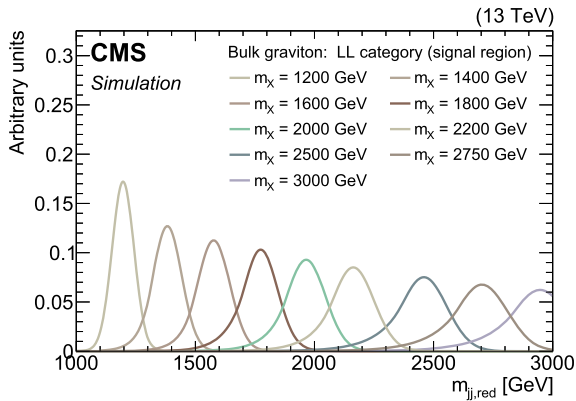


Fig. 4. The bulk graviton signal $m_{jj,\text{red}}$ distribution for the LL category, modelled using the sum of Gaussian and Crystal Ball functions. This modelling is performed for signals in the range $1100 < m_{jj,\text{red}} < 3000$ GeV, where the background distribution falls smoothly. No events are observed with $m_{jj,\text{red}}$ greater than 3000 GeV.

Table 1

Definition of the signal, the antitag, and the sideband regions used for the background estimation. The regions are defined in terms of the soft-drop masses of the leading p_T (j_1) and the subleading p_T (j_2) AK8 jets, and their double-b tagger discriminator values.

Event category	Jet	Soft-drop mass (GeV)	Double-b tagger discriminator
Signal (LL)	j_1		>0.3 , but
	j_2	105–135	not both >0.8
Signal (TT)	j_1		>0.8
	j_2		
Antitag (LL)	j_1		<0.3
	j_2	105–135	0.3–0.8
Antitag (TT)	j_1		<0.3
	j_2		>0.8
Sideband (LL, passing)	j_1	<105 or >135	>0.3 , but
	j_2	105–135	not both >0.8
Sideband (TT, passing)	j_1	<105 or >135	>0.8
	j_2	105–135	
Sideband (LL, failing)	j_1	<105 or >135	<0.3
	j_2	105–135	0.3–0.8
Sideband (TT, failing)	j_1	<105 or >135	<0.3
	j_2	105–135	>0.8

is estimated in bins of the $m_{jj,\text{red}}$ distribution. Considering these two variables, several regions are defined.

The *pre-tag* region includes events fulfilling the selection requirements in Sections 2–3 apart from those on m_{j_1} and on the j_1 double-b tagger discriminator. The *signal* region is the subset of pre-tag events where m_{j_1} is inside the H jet mass window of 105–135 GeV, and with the j_1 double-b tagger discriminator greater than 0.3 or 0.8, for the LL and TT regions, respectively. The *antitag* regions require the j_1 double-b tagger discriminator to be less than 0.3, with the requirement on j_2 being the same as that for the corresponding LL or TT signal regions. The m_{j_1} *sideband* region consists of events in the pre-tag region, where m_{j_1} lies outside the H jet mass window. Based on whether j_1 passes or fails the double-b tagger discriminator threshold, the sideband region is divided into either “passing” or “failing”, respectively. The antitag regions are dominated by the multijet background, and have identical kinematic distributions to the multijet background events in the signal region, according to studies using simulations. The definitions of the signal, the antitag, and the sideband regions are given in Table 1.

In the absence of a correlation between m_{j_1} and the double-b tagger discriminator values, one could measure in the m_{j_1} sideband the ratio of the number of events passing and failing the

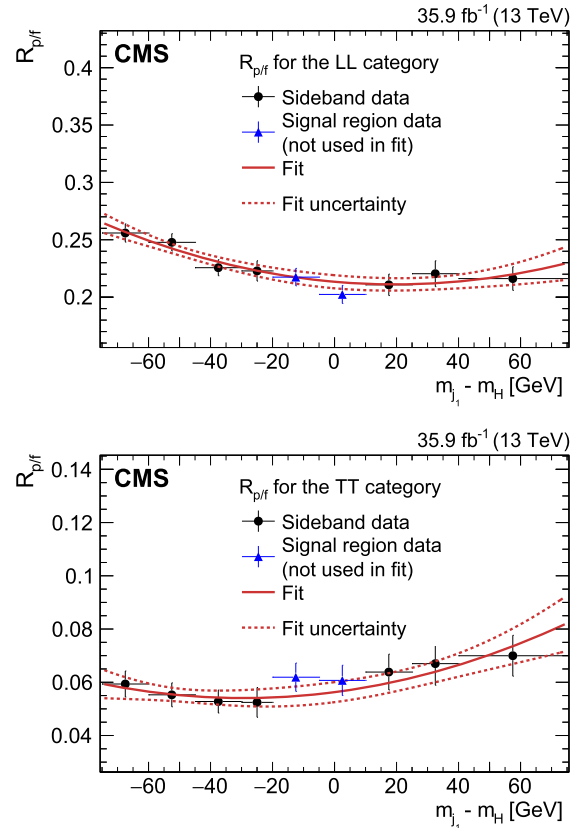


Fig. 5. The pass-fail ratio $R_{p/f}$ of the leading p_T jet for the LL (upper) and TT (lower) signal region categories as a function of the difference between the soft-drop mass of the leading jet and the Higgs boson mass, $m_{j_1} - m_H$. The measured ratio in different bins of $m_{j_1} - m_H$ is used in the fit (red solid line), except in the region around $m_{j_1} - m_H = 0$, which corresponds to the signal region (blue triangular markers). The fitted function is interpolated to obtain $R_{p/f}$ in the signal region. The horizontal bars on the data points indicate the bin widths. (For interpretation of the colours in the figure(s), the reader is referred to the web version of this article.)

double-b tagger selection, $R_{p/f} \equiv N_{\text{pass}}/N_{\text{fail}}$, i.e. the “pass-fail ratio”. The yield in the antitag region (in each $m_{jj,\text{red}}$ bin) could then be scaled by $R_{p/f}$ to obtain an estimate of the background normalization in the signal region. However, there is a small correlation between the double-b tagger discriminator and m_{j_1} , which is taken into account by measuring the pass-fail ratio $R_{p/f}$ as a function of m_{j_1} . The signal fraction was found to be less than 10^{-3} in the sideband regions used to evaluate $R_{p/f}$, assuming a signal cross section $\sigma(\text{pp} \rightarrow X \rightarrow \text{HH} \rightarrow \text{bbbb})$ of 10 fb.

The $R_{p/f}$ for the LL signal region is measured using ratio of the number of events in the “LL, passing” and “LL, failing” sideband regions, as defined in Table 1. Likewise, the $R_{p/f}$ for the TT signal region uses the ratio of the number of events in the “TT, passing” to the “TT, failing” sideband regions. The variation of $R_{p/f}$ as a function of m_{j_1} in each m_{j_1} sideband is fitted with a quadratic function. The fit to the pass-fail ratio is interpolated to the region where m_{j_1} lies within the H jet mass window of 105–135 GeV. An alternative fit using a third order polynomial was found to give the same interpolated value of $R_{p/f}$ in the Higgs jet mass window. Every event in the antitag region is scaled by the pass-fail ratio evaluated for the m_{j_1} of that event, to obtain the background prediction in the signal region.

Fig. 5 shows the quadratic fit in the m_{j_1} sidebands of the pass-fail ratio $R_{p/f}$ as a function of m_{j_1} , as obtained in the data. The background prediction using this method, along with the number of observed events in the signal region is shown in Fig. 6.

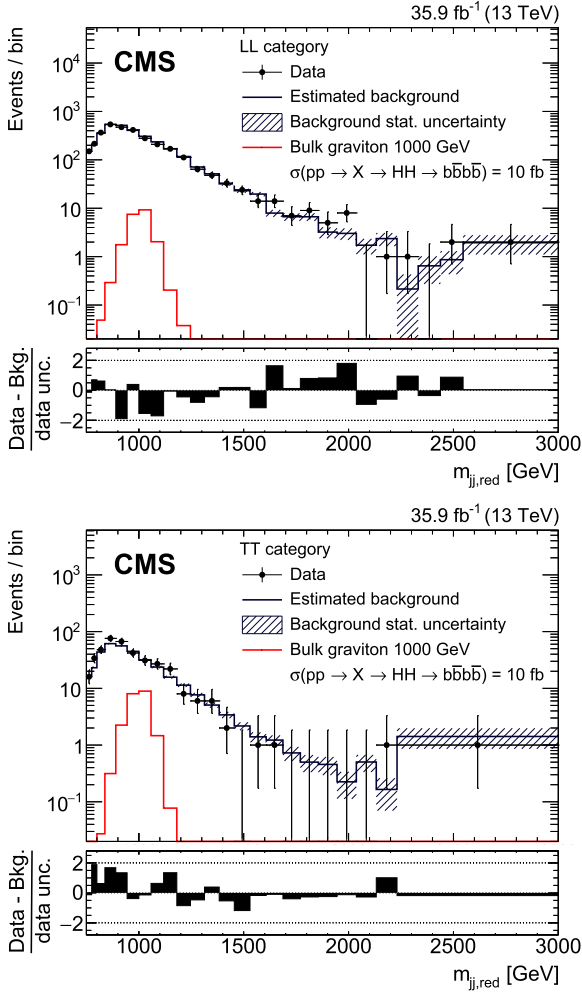


Fig. 6. The reduced mass distributions $m_{jj,red}$ for the LL (upper) and TT (lower) signal region categories. The points with bars show the data, the histogram with shaded band shows the estimated background and associated uncertainty. The $m_{jj,red}$ spectrum for the background is obtained by weighting the $m_{jj,red}$ spectrum in the antitag region by the ratio $R_{p/f}$ of Fig. 5. The signal predictions for a bulk graviton of mass 1000 GeV, are overlaid for comparison, assuming a cross section $\sigma(pp \rightarrow X \rightarrow HH \rightarrow b\bar{b}b\bar{b})$ of 10 fb. The last bins of the distributions contain all events with $m_{jj,red} > 3000$ GeV. The differences between the data and the predicted background, divided by the data statistical uncertainty (data unc.) as given by the Garwood interval [76], are shown in the lower panels.

For resonance masses of 1200 GeV and above, the background estimation is improved by simultaneously fitting a parametric model for the background and signal to the data in the signal and the antitag regions for $m_{jj,red} \geq 1100$ GeV. In the fit, the ratio $R_{p/f}$ obtained from the sidebands is used to constrain the relative number of background events in the two regions. To account for possible $R_{p/f}$ dependence on $m_{jj,red}$ at high $m_{jj,red}$ values, the $R_{p/f}$ obtained from the fits shown in Fig. 5 is also parametrized as a linear function of $m_{jj,red}$. The signal normalization is unconstrained in the fit, while the uncertainties in the parameters of the functions used to model the background and $R_{p/f}$ are treated as nuisance parameters. For the background modelling, a choice among an exponential function $Ne^{-am_{jj,red}}$, a “levelled exponential” function $Ne^{-am_{jj,red}/(1+bm_{jj,red})}$, and a “quadratic levelled exponential function” $Ne^{[-am_{jj,red}/(1+bm_{jj,red})] - [cm_{jj,red}^2/(1+cm_{jj,red}^2)]}$ was made, using a Fisher F-test [77]. At a confidence level of 95%, the levelled exponential function was found to be optimal. Since the background shapes in the signal regions, as predicted using the antitag re-

gions, were found to be similar (Fig. 6), the parametric background modelling was tested using the antitag region in the data before applying it to the signal region.

The simultaneous fits to the antitag and the signal regions are shown in Figs. 7 and 8, respectively, using the background model only. These are labelled as “post-fit” curves with the signal region background yields constrained to be $R_{p/f}$ times the background yields from the antitag regions. The “pre-fit” curves, obtained by fitting the antitag and the signal regions separately to the background-only model, with the background event yields unconstrained, are also shown for comparison. In the post-fit results, the $R_{p/f}$ dependence on $m_{jj,red}$ was found to be negligible.

Among the four fitted regions, corresponding to the antitag and the signal regions in the LL and TT categories, the events with the highest value of $m_{jj,red}$ occur in the antitag region of the LL category, at around $m_{jj,red} = 2850$ GeV. As the parametric background model is only reliable within the range of observed events, the likelihood is only evaluated up to $m_{jj,red} = 3000$ GeV. This results in a truncation of the signal distribution for resonances having m_χ of 2800 GeV and above, with signal efficiency losses increasing to 30% for $m_\chi = 3000$ GeV, as shown in Fig. 4.

Closure tests of the background estimation methods were performed using simulated multijet samples with signals of various cross sections. The tests indicated a good consistency between the expected and the assumed signal strengths.

5. Systematic uncertainties

The following sources of systematic uncertainty affect the expected signal yields. None of these lead to a significant change in the signal shape.

Trigger response modelling uncertainties are particularly important for $m_{jj,red} < 1200$ GeV, where the trigger efficiency drops below 99%. A scale factor is applied to correct for the difference in efficiency observed between the data and simulation. The control trigger used to measure this scale factor requires a single AK4 jet with $p_T > 260$ GeV, and it too is subject to some inefficiency when $m_{jj,red}$ is close to 750 GeV, because of a difference between the jet energy scale used in the trigger and that used in the offline reconstruction. This inefficiency is measured using simulations, and has an associated total uncertainty of between 1% and 15%.

The jet energy scale and resolution uncertainty is about 1% [63, 64]. The jet mass scale and resolution, and τ_{21} selection efficiency data-to-simulation scale factor are measured using a sample of merged W jets in semileptonic $t\bar{t}$ events. The corresponding uncertainties are extrapolated to a higher p_T range than that associated with $t\bar{t}$ events, using simulations. A correction factor is applied to account for the difference in the jet shower profile of $W \rightarrow q\bar{q}'$ and $H \rightarrow b\bar{b}$ decays, by comparing the ratio of the efficiency of H and W jets using the PYTHIA 8 and HERWIG++ shower generators. The jet mass scale and resolution has a 2% effect on the signal yields because of a change in the mean of the H jet mass distribution. The τ_{21} selection efficiency uncertainty amounts to a +30/−26% change in the signal yields. The uncertainty in the H tagging correction factor is in the range 7–20% depending on the resonance mass m_χ . The double-b tagger efficiency scale factor uncertainty is about 2–5%, depending on the double-b tagger requirement threshold and jet p_T , and is propagated to the total uncertainty in the signal yield.

The impact of the PDFs and the theoretical scale uncertainties are estimated to be 0.1–2%, using the PDF4LHC procedure [50], and affect the product of the signal acceptance and the efficiency. The PDF and scale uncertainties have negligible impact on the signal $m_{jj,red}$ distributions. Additional systematic uncertainties associated

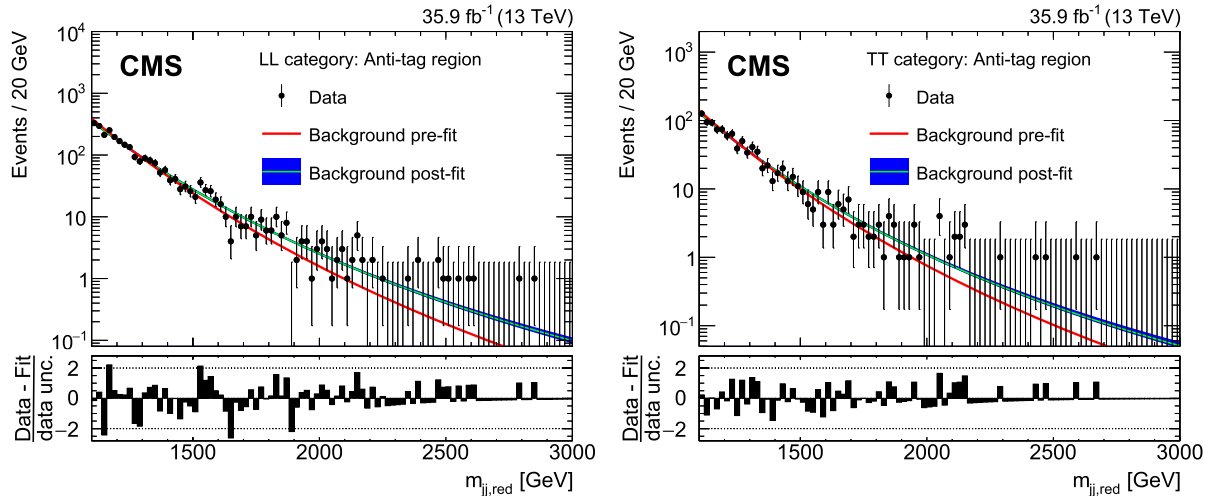


Fig. 7. The reduced mass $m_{jj,red}$ distributions in the antitag region for the LL (left) and TT (right) categories. The black markers are the data while the curves show the pre-fit and post-fit background shapes. The differences between the data and the pre-fit background distribution, divided by the statistical uncertainty in the data (data unc.) as given by the Garwood interval [76], are shown in the lower panels.

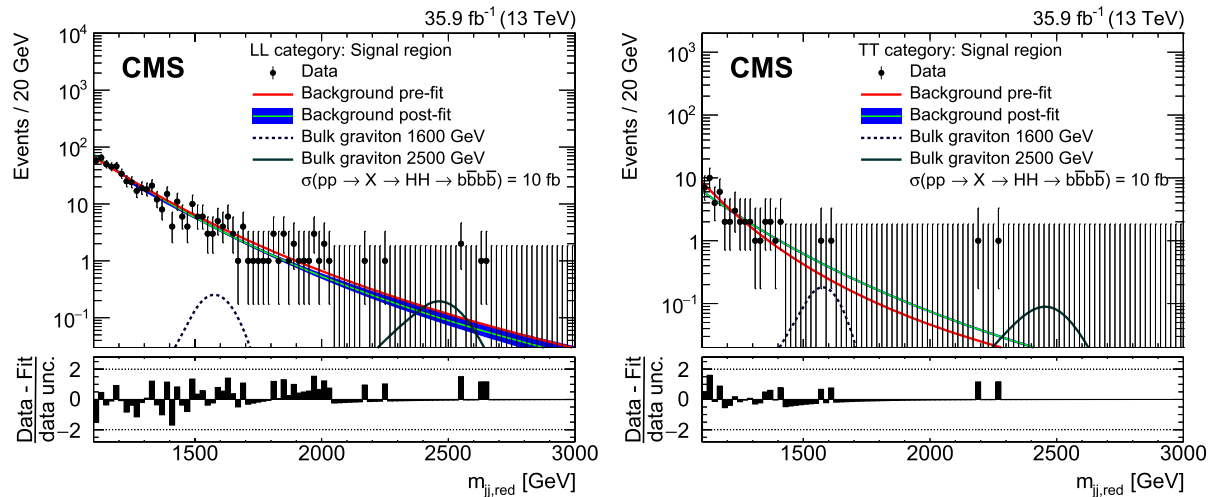


Fig. 8. The reduced mass $m_{jj,red}$ distributions in the signal region for the LL (left) and the TT (right) categories. The black markers are the data while the curves show the pre-fit and post-fit background shapes. The contribution of bulk gravitons of masses 1600 and 2500 GeV in the signal region are shown assuming a cross section $\sigma(pp \rightarrow X \rightarrow HH \rightarrow b\bar{b}b\bar{b})$ of 10 fb. The differences between the data and the pre-fit background distribution, divided by the statistical uncertainty in the data (data unc.) as given by the Garwood interval [76], are shown in the lower panels.

with the pileup modelling (2%) and the integrated luminosity determination (2.5%) [78], are applied to the signal yield.

The main source of uncertainty for the multijet background in the region $m_{jj,red} < 1200 \text{ GeV}$ is due to the statistical uncertainty in the fit to the $R_{p/f}$ ratio performed in the H jet mass sidebands. This uncertainty, amounting to 2.6% for the LL, and 6.8% for the TT signal categories, is fully correlated between all bins of a particular estimate. Furthermore, the statistical uncertainty in the antitag region is propagated to the signal region when the estimate is made. This is uncorrelated from bin to bin, and the Barlow–Beeston Lite [79,80] method is used to treat the bin-by-bin statistical uncertainty in the data. These uncertainties affect both the shape of the background in the $m_{jj,red}$ distribution and the total background yield.

For $m_{jj,red} \geq 1200 \text{ GeV}$, the overall background uncertainty is obtained from the uncertainty in the four simultaneous fits performed for the antitag and the signal regions in the LL and the

Table 2

Summary of systematic uncertainties in the signal and background yields.

Source	Uncertainty (%)
Signal yield	
Trigger efficiency	1–15
H jet energy scale and resolution	1
H jet mass scale and resolution	2
H jet τ_{21} selection	+30/–26
H-tagging correction factor	7–20
Double-b tagger discriminator	2–5
Pileup modelling	2
PDF and scales	0.1–2
Luminosity	2.5
Background yield	
$R_{p/f}$ fit	2.6 (LL category) 6.8 (TT category)

TT categories. The dependence of $R_{p/f}$ on $m_{jj,red}$ is accounted for, although this was found to be negligible.

A complete list of systematic uncertainties is given in Table 2.

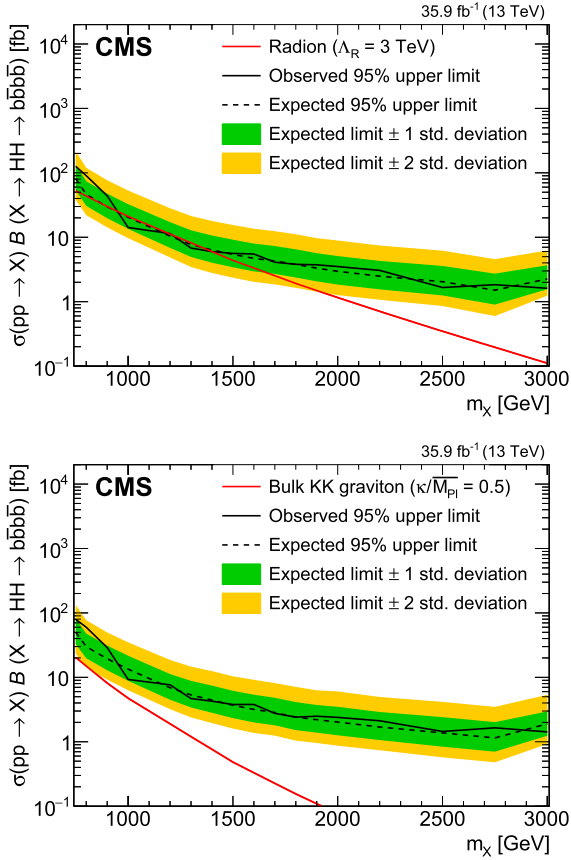


Fig. 9. The limits for the spin-0 radion (upper) and the spin-2 bulk graviton (lower) models. The result for $m_X < 1200$ GeV uses the background predicted using the control regions, while for $m_X \geq 1200$ GeV the background is derived from a combined signal and background fit to the data in the control and the signal regions. The predicted theoretical cross sections for a narrow radion or a bulk graviton are also shown.

6. Results

As shown in Figs. 6 and 8, for the signal regions, the observed $m_{j_i, \text{red}}$ distribution is consistent with the estimated background. The results are interpreted in terms of upper limits on the product of the production cross sections and the branching fractions $\sigma(pp \rightarrow X)\mathcal{B}(X \rightarrow HH \rightarrow b\bar{b}b\bar{b})$ for radion and bulk graviton of various mass hypotheses. The asymptotic approximation of the modified frequentist approach for confidence levels, taking the profile likelihood as a test statistic [81–83], is used. The limits are shown in Fig. 9 for a narrow width radion or a bulk graviton. These are compared with the theoretical values of the product of the cross sections and branching fractions for the benchmarks $\kappa/\overline{M}_{\text{Pl}} = 0.5$ and $\Lambda_R = 3$ TeV, where the narrow width approximation for a signal is valid, and where the corresponding HH decay branching fractions in the mass range of interest are 10 and 23%, for the graviton and the radion, respectively [13]. The expected limits on the bulk graviton are more stringent than those on the radion because of the higher efficiency of the $|\Delta\eta(j_1, j_2)|$ separation requirement for the former signal.

The upper limits on the production of the cross sections and branching fraction lies in the range 126–1.4 fb for a narrow resonance X of mass $750 < m_X < 3000$ GeV. Assuming $\Lambda_R = 3$ TeV, a bulk radion with a mass between 970 and 1400 GeV is excluded at 95% confidence level, except in a small region close to 1200 GeV, where the observed limit is 11.4 pb, the theoretical prediction being 11.2 pb.

7. Summary

A search for a narrow massive resonance decaying to two standard model Higgs bosons is performed using the LHC proton–proton collision data collected at a centre-of-mass energy of 13 TeV by the CMS detector, and corresponding to an integrated luminosity of 35.9 fb^{-1} . The final state consists of events with both Higgs bosons decaying to b quark–antiquark pairs, which were identified using jet substructure and b-tagging techniques applied to large-area jets. The data are found to be consistent with the standard model expectations, dominated by multijet events. Upper limits are set on the products of the resonant production cross sections of a Kaluza–Klein bulk graviton and a Randall–Sundrum radion, and their branching fraction to $HH \rightarrow b\bar{b}b\bar{b}$. The limits range from 126 to 1.4 fb at 95% confidence level for bulk gravitons and radions in the mass range 750–3000 GeV. For the mass scale $\Lambda_R = 3$ TeV, a radion of mass between 970 and 1400 GeV (except in a small region close to 1200 GeV) is excluded. These limits on the bulk graviton and the radion decaying to a pair of standard model Higgs bosons are the most stringent to date, over the mass range explored.

Acknowledgements

We congratulate our colleagues in the CERN accelerator departments for the excellent performance of the LHC and thank the technical and administrative staffs at CERN and at other CMS institutes for their contributions to the success of the CMS effort. In addition, we gratefully acknowledge the computing centres and personnel of the Worldwide LHC Computing Grid for delivering so effectively the computing infrastructure essential to our analyses. Finally, we acknowledge the enduring support for the construction and operation of the LHC and the CMS detector provided by the following funding agencies: BMWFW and FWF (Austria); FNRS and FWO (Belgium); CNPq, CAPES, FAPERJ, and FAPESP (Brazil); MES (Bulgaria); CERN; CAS, MOST, and NSFC (China); COLCIENCIAS (Colombia); MSES and CSF (Croatia); RPF (Cyprus); SENESCYT (Ecuador); MoER, ERC IUT, and ERDF (Estonia); Academy of Finland, MEC, and HIP (Finland); CEA and CNRS/IN2P3 (France); BMBF, DFG, and HGF (Germany); GSRT (Greece); OTKA and NIH (Hungary); DAE and DST (India); IPM (Iran); SFI (Ireland); INFN (Italy); MSIP and NRF (Republic of Korea); LAS (Lithuania); MOE and UM (Malaysia); BUAP, CINVESTAV, CONACYT, LNS, SEP, and UASLP-FAI (Mexico); MBIE (New Zealand); PAEC (Pakistan); MSHE and NSC (Poland); FCT (Portugal); JINR (Dubna); MON, ROSATOM, RAS, RFBR and RAEP (Russia); MESTD (Serbia); SEIDI, CPAN, PCTI and FEDER (Spain); Swiss Funding Agencies (Switzerland); MST (Taipei); ThEP-Center, IPST, STAR, and NSTDA (Thailand); TUBITAK and TAEK (Turkey); NASU and SFFR (Ukraine); STFC (United Kingdom); DOE and NSF (USA).

Individuals have received support from the Marie-Curie programme and the European Research Council and Horizon 2020 Grant, contract No. 675440 (European Union); the Leventis Foundation; the A. P. Sloan Foundation; the Alexander von Humboldt Foundation; the Belgian Federal Science Policy Office; the Fonds pour la Formation à la Recherche dans l'Industrie et dans l'Agriculture (FRIA-Belgium); the Agentschap voor Innovatie door Wetenschap en Technologie (IWT-Belgium); the Ministry of Education, Youth and Sports (MEYS) of the Czech Republic; the Council of Science and Industrial Research, India; the HOMING PLUS programme of the Foundation for Polish Science, cofinanced from European Union, Regional Development Fund, the Mobility Plus programme of the Ministry of Science and Higher Education, the National Science Center (Poland), contracts Harmonia 2014/14/M/ST2/00428, Opus 2014/13/B/ST2/02543, 2014/15/B/ST2/03998, and 2015/19/

B/ST2/02861, Sonata-bis 2012/07/E/ST2/01406; the National Priorities Research Program by Qatar National Research Fund; the Programa Severo Ochoa del Principado de Asturias; the Thalís and Aristeia programmes cofinanced by EU-ESF and the Greek NSRF; the Rachadapisek Sompot Fund for Postdoctoral Fellowship, Chulalongkorn University and the Chulalongkorn Academic into Its 2nd Century Project Advancement Project (Thailand); the Welch Foundation, contract C-1845; and the Weston Havens Foundation (USA).

References

- [1] ATLAS Collaboration, Observation of a new particle in the search for the Standard Model Higgs boson with the ATLAS detector at the LHC, Phys. Lett. B 716 (2012) 01, <https://doi.org/10.1016/j.physletb.2012.08.020>, arXiv:1207.7214.
- [2] CMS Collaboration, Observation of a new boson at a mass of 125 GeV with the CMS experiment at the LHC, Phys. Lett. B 716 (2012) 30, <https://doi.org/10.1016/j.physletb.2012.08.021>, arXiv:1207.7235.
- [3] CMS Collaboration, Observation of a new boson with mass near 125 GeV in pp collisions at $\sqrt{s} = 7$ and 8 TeV, J. High Energy Phys. 06 (2013) 081, [https://doi.org/10.1007/JHEP06\(2013\)081](https://doi.org/10.1007/JHEP06(2013)081), arXiv:1303.4571.
- [4] D. de Florian, J. Mazzitelli, Higgs boson pair production at next-to-next-to-leading order in QCD, Phys. Rev. Lett. 111 (2013) 201801, <https://doi.org/10.1103/PhysRevLett.111.201801>, arXiv:1309.6594.
- [5] L. Randall, R. Sundrum, A large mass hierarchy from a small extra dimension, Phys. Rev. Lett. 83 (1999) 3370, <https://doi.org/10.1103/PhysRevLett.83.3370>, arXiv:hep-ph/9905221.
- [6] W.D. Goldberger, M.B. Wise, Modulus stabilization with bulk fields, Phys. Rev. Lett. 83 (1999) 4922, <https://doi.org/10.1103/PhysRevLett.83.4922>, arXiv:hep-ph/9907447.
- [7] C. Csaki, M. Graesser, L. Randall, J. Terning, Cosmology of brane models with radion stabilization, Phys. Rev. D 62 (2000) 045015, <https://doi.org/10.1103/PhysRevD.62.045015>, arXiv:hep-ph/9911406.
- [8] C. Csaki, M.L. Graesser, G.D. Kribs, Radion dynamics and electroweak physics, Phys. Rev. D 63 (2001) 065002, <https://doi.org/10.1103/PhysRevD.63.065002>, arXiv:hep-th/0008151.
- [9] H. Davoudiasl, J.L. Hewett, T.G. Rizzo, Phenomenology of the Randall–Sundrum gauge hierarchy model, Phys. Rev. Lett. 84 (2000) 2080, <https://doi.org/10.1103/PhysRevLett.84.2080>, arXiv:hep-ph/9909255.
- [10] O. DeWolfe, D.Z. Freedman, S.S. Gubser, A. Karch, Modeling the fifth dimension with scalars and gravity, Phys. Rev. D 62 (2000) 046008, <https://doi.org/10.1103/PhysRevD.62.046008>, arXiv:hep-th/9909134.
- [11] K. Agashe, H. Davoudiasl, G. Perez, A. Soni, Warped gravitons at the LHC and beyond, Phys. Rev. D 76 (2007) 036006, <https://doi.org/10.1103/PhysRevD.76.036006>, arXiv:hep-ph/0701186.
- [12] G.F. Giudice, R. Rattazzi, J.D. Wells, Gravitons from higher dimensional metrics and curvature Higgs mixing, Nucl. Phys. B 595 (2001) 250, [https://doi.org/10.1016/S0550-3213\(00\)00686-6](https://doi.org/10.1016/S0550-3213(00)00686-6), arXiv:hep-ph/0002178.
- [13] A. Oliveira, Gravity particles from warped extra dimensions, a review. Part I – KK graviton, arXiv:1404.0102, 2014.
- [14] G.C. Branco, P.M. Ferreira, L. Lavoura, M.N. Rebelo, M. Sher, J.P. Silva, Theory and phenomenology of two-Higgs-doublet models, Phys. Rep. 516 (2012) 01, <https://doi.org/10.1016/j.physrep.2012.02.002>, arXiv:1106.0034.
- [15] A. Djouadi, The anatomy of electroweak symmetry breaking. Tome II: the Higgs bosons in the minimal supersymmetric model, Phys. Rep. 459 (2008) 01, <https://doi.org/10.1016/j.physrep.2007.10.005>, arXiv:hep-ph/0503173.
- [16] H. Georgi, M. Machacek, Doubly charged Higgs bosons, Nucl. Phys. B 262 (1985) 463, [https://doi.org/10.1016/0550-3213\(85\)90325-6](https://doi.org/10.1016/0550-3213(85)90325-6).
- [17] ATLAS Collaboration, Search for Higgs boson pair production in the $\gamma\gamma b\bar{b}$ final state using pp collision data at $\sqrt{s} = 8$ TeV from the ATLAS detector, Phys. Rev. Lett. 114 (2015) 081802, <https://doi.org/10.1103/PhysRevLett.114.081802>, arXiv:1406.5053.
- [18] ATLAS Collaboration, Search for Higgs boson pair production in the $b\bar{b}b\bar{b}$ final state from pp collisions at $\sqrt{s} = 8$ TeV with the ATLAS detector, Eur. Phys. J. C 75 (2015) 412, <https://doi.org/10.1140/epjc/s10052-015-3628-x>, arXiv:1506.00285.
- [19] ATLAS Collaboration, Searches for Higgs boson pair production in the $hh \rightarrow b\bar{b}\tau\tau, \gamma\gamma WW^*, \gamma\gamma b\bar{b}, b\bar{b}b\bar{b}$ channels with the ATLAS detector, Phys. Rev. D 92 (2015) 092004, <https://doi.org/10.1103/PhysRevD.92.092004>, arXiv:1509.04670.
- [20] CMS Collaboration, Searches for heavy Higgs bosons in two-Higgs-doublet models and for $t \rightarrow ch$ decay using multilepton and diphoton final states in pp collisions at 8 TeV, Phys. Rev. D 90 (2014) 112013, <https://doi.org/10.1103/PhysRevD.90.112013>, arXiv:1410.2751.
- [21] CMS Collaboration, Search for resonant pair production of Higgs bosons decaying to two bottom quark–antiquark pairs in proton–proton collisions at 8 TeV, Phys. Lett. B 749 (2015) 560, <https://doi.org/10.1016/j.physletb.2015.08.047>, arXiv:1503.04114.
- [22] CMS Collaboration, Searches for a heavy scalar boson H decaying to a pair of 125 GeV Higgs bosons hh or for a heavy pseudoscalar boson A decaying to Zh, in the final states with $h \rightarrow \tau\tau$, Phys. Lett. B 755 (2016) 217, <https://doi.org/10.1016/j.physletb.2016.01.056>, arXiv:1510.01181.
- [23] CMS Collaboration, Search for two Higgs bosons in final states containing two photons and two bottom quarks in proton–proton collisions at 8 TeV, Phys. Rev. D 94 (2016) 052012, <https://doi.org/10.1103/PhysRevD.94.052012>, arXiv:1603.06896.
- [24] CMS Collaboration, Search for heavy resonances decaying to two Higgs bosons in final states containing four b quarks, Eur. Phys. J. C 76 (2016) 371, <https://doi.org/10.1140/epjc/s10052-016-4206-6>, arXiv:1602.08762.
- [25] ATLAS Collaboration, Search for pair production of Higgs bosons in the $b\bar{b}b\bar{b}$ final state using proton–proton collisions at $\sqrt{s} = 13$ TeV with the ATLAS detector, Phys. Rev. D 94 (2016) 052002, <https://doi.org/10.1103/PhysRevD.94.052002>, arXiv:1606.04782.
- [26] ATLAS Collaboration, Search for high-mass diboson resonances with boson-tagged jets in proton–proton collisions at $\sqrt{s} = 8$ TeV with the ATLAS detector, J. High Energy Phys. 12 (2015) 055, [https://doi.org/10.1007/JHEP12\(2015\)055](https://doi.org/10.1007/JHEP12(2015)055), arXiv:1506.00962.
- [27] ATLAS Collaboration, Search for production of WW/WZ resonances decaying to a lepton, neutrino and jets in pp collisions at $\sqrt{s} = 8$ TeV with the ATLAS detector, Eur. Phys. J. C 75 (2015) 209, <https://doi.org/10.1140/epjc/s10052-015-3425-6>, arXiv:1503.04677, Erratum: <https://doi.org/10.1140/epjc/s10052-015-3593-4>.
- [28] ATLAS Collaboration, Search for resonant diboson production in the $\ell\ell q\bar{q}$ final state in pp collisions at $\sqrt{s} = 8$ TeV with the ATLAS detector, Eur. Phys. J. C 75 (2015) 69, <https://doi.org/10.1140/epjc/s10052-015-3261-8>, arXiv:1409.6190.
- [29] CMS Collaboration, Search for massive resonances in dijet systems containing jets tagged as W or Z boson decays in pp collisions at $\sqrt{s} = 8$ TeV, J. High Energy Phys. 08 (2014) 173, [https://doi.org/10.1007/JHEP08\(2014\)173](https://doi.org/10.1007/JHEP08(2014)173), arXiv:1405.1994.
- [30] CMS Collaboration, Search for massive resonances decaying into pairs of boosted bosons in semi-leptonic final states at $\sqrt{s} = 8$ TeV, J. High Energy Phys. 08 (2014) 174, [https://doi.org/10.1007/JHEP08\(2014\)174](https://doi.org/10.1007/JHEP08(2014)174), arXiv:1405.3447.
- [31] ATLAS Collaboration, Search for diboson resonances with boson-tagged jets in pp collisions at $\sqrt{s} = 13$ TeV with the ATLAS detector, Phys. Lett. B 777 (2018) 91, <https://doi.org/10.1016/j.physletb.2017.12.011>, arXiv:1708.04445.
- [32] ATLAS Collaboration, Search for WW/WZ resonance production in $\ell\nu q\bar{q}$ final states in pp collisions at $\sqrt{s} = 13$ TeV with the ATLAS detector, J. High Energy Phys. 03 (2017) 042, [https://doi.org/10.1007/JHEP03\(2017\)042](https://doi.org/10.1007/JHEP03(2017)042), arXiv:1710.07235.
- [33] ATLAS Collaboration, Searches for heavy ZZ and ZW resonances in the $\ell\ell q\bar{q}$ and $\nu\nu q\bar{q}$ final states in pp collisions at $\sqrt{s} = 13$ TeV with the ATLAS detector, J. High Energy Phys. 03 (2018) 009, [https://doi.org/10.1007/JHEP03\(2018\)009](https://doi.org/10.1007/JHEP03(2018)009), arXiv:1708.09638, 2017.
- [34] CMS Collaboration, Combination of searches for heavy resonances decaying to WW, WZ, ZZ, and ZH boson pairs in proton–proton collisions at $\sqrt{s} = 8$ and 13 TeV, Phys. Lett. B 774 (2017) 533, <https://doi.org/10.1016/j.physletb.2017.09.083>, arXiv:1705.09171.
- [35] CMS Collaboration, Search for massive resonances decaying into WW, WZ, ZZ, qW, and qZ with dijet final states at $\sqrt{s} = 13$ TeV, arXiv:1708.05379, Phys. Rev. D (2018), submitted for publication.
- [36] D. de Florian, et al., Handbook of LHC Higgs Cross Sections: 4. Deciphering the Nature of the Higgs Sector, CERN Report CERN-2017-002-M, CERN, 2016, <https://doi.org/10.23731/CYRM-2017-002>, arXiv:1610.07922.
- [37] J.M. Butterworth, A.R. Davison, M. Rubin, G.P. Salam, Jet substructure as a new Higgs search channel at the LHC, Phys. Rev. Lett. 100 (2008) 242001, <https://doi.org/10.1103/PhysRevLett.100.242001>, arXiv:0802.2470.
- [38] B. Cooper, N. Konstantinidis, L. Lambourne, D. Wardrope, Boosted $hh \rightarrow b\bar{b}b\bar{b}$: a new topology in searches for TeV-scale resonances at the LHC, Phys. Rev. D 88 (2013) 114005, <https://doi.org/10.1103/PhysRevD.88.114005>, arXiv:1307.0407.
- [39] M. Gouzevitch, A. Oliveira, J. Rojo, R. Rosenfeld, G.P. Salam, V. Sanz, Scale-invariant resonance tagging in multijet events and new physics in Higgs pair production, J. High Energy Phys. 07 (2013) 148, [https://doi.org/10.1007/JHEP07\(2013\)148](https://doi.org/10.1007/JHEP07(2013)148), arXiv:1303.6636.
- [40] CMS Collaboration, The CMS experiment at the CERN LHC, J. Instrum. 3 (2008) S08004, <https://doi.org/10.1088/1748-0221/3/08/S08004>.
- [41] CMS Collaboration, The CMS trigger system, J. Instrum. 12 (2017) P01020, <https://doi.org/10.1088/1748-0221/12/01/P01020>, arXiv:1609.02366.
- [42] CMS Collaboration, Particle-flow reconstruction and global event description with the CMS detector, J. Instrum. 12 (2017) P10003, <https://doi.org/10.1088/1748-0221/12/10/P10003>, arXiv:1706.04965.
- [43] M. Cacciari, G.P. Salam, G. Soyez, The anti- k_r jet clustering algorithm, J. High Energy Phys. 04 (2008) 063, <https://doi.org/10.1088/1126-6708/2008/04/063>, arXiv:0802.1189.
- [44] M. Cacciari, G.P. Salam, G. Soyez, FastJet user manual, Eur. Phys. J. C 72 (2012) 1896, <https://doi.org/10.1140/epjc/s10052-012-1896-2>, arXiv:1111.6097.
- [45] J. Alwall, R. Frederix, S. Frixione, V. Hirschi, F. Maltoni, O. Mattelaer, H.S. Shao, T. Stelzer, P. Torrielli, M. Zaro, The automated computation of tree-level and next-to-leading order differential cross sections, and their matching

- to parton shower simulations, *J. High Energy Phys.* 07 (2014) 079, [https://doi.org/10.1007/JHEP07\(2014\)079](https://doi.org/10.1007/JHEP07(2014)079), arXiv:1405.0301.
- [46] R.D. Ball, et al., NNPDF Collaboration, Parton distributions for the LHC Run II, *J. High Energy Phys.* 04 (2015) 040, [https://doi.org/10.1007/JHEP04\(2015\)040](https://doi.org/10.1007/JHEP04(2015)040), arXiv:1410.8849.
- [47] L.A. Harland-Lang, A.D. Martin, P. Motylinski, R.S. Thorne, Parton distributions in the LHC era: MMHT 2014 PDFs, *Eur. Phys. J. C* 75 (2015) 204, <https://doi.org/10.1140/epjc/s10052-015-3397-6>, arXiv:1412.3989.
- [48] A. Buckley, J. Ferrando, S. Lloyd, K. Nordström, B. Page, M. Rüfenacht, M. Schönherr, G. Watt, LHAPDF6: parton density access in the LHC precision era, *Eur. Phys. J. C* 75 (2015) 132, <https://doi.org/10.1140/epjc/s10052-015-3318-8>, arXiv:1412.7420.
- [49] S. Carrazza, J.I. Latorre, J. Rojo, G. Watt, A compression algorithm for the combination of PDF sets, *Eur. Phys. J. C* 75 (2015) 474, <https://doi.org/10.1140/epjc/s10052-015-3703-3>, arXiv:1504.06469.
- [50] J. Butterworth, et al., PDF4LHC recommendations for LHC Run II, *J. Phys. G* 43 (2016) 023001, <https://doi.org/10.1088/0954-3899/43/2/023001>, arXiv:1510.03865.
- [51] T. Sjöstrand, S. Ask, J.R. Christiansen, R. Corke, N. Desai, P. Ilten, S. Mrenna, S. Prestel, C.O. Rasmussen, P.Z. Skands, An Introduction to PYTHIA 8.2, *Comput. Phys. Commun.* 191 (2015) 159, <https://doi.org/10.1016/j.cpc.2015.01.024>, arXiv:1410.3012.
- [52] M. Bähr, S. Gieseke, M.A. Gigg, D. Grellscheid, K. Hamilton, O. Latunde-Dada, S. Plätzer, P. Richardson, M.H. Seymour, A. Sherstnev, B.R. Webber, Herwig++ physics and manual, *Eur. Phys. J. C* 58 (2008) 639, <https://doi.org/10.1140/epjc/s10052-008-0798-9>, arXiv:0803.0883.
- [53] CMS Collaboration, Event generator tunes obtained from underlying event and multiparton scattering measurements, *Eur. Phys. J. C* 76 (2016) 155, <https://doi.org/10.1140/epjc/s10052-016-3988-x>, arXiv:1512.00815.
- [54] S. Gieseke, C. Rohr, A. Siodmok, Colour reconstructions in Herwig++, *Eur. Phys. J. C* 72 (2012) 2225, <https://doi.org/10.1140/epjc/s10052-012-2225-5>, arXiv:1206.0041.
- [55] S. Frixione, G. Ridolfi, P. Nason, A positive-weight next-to-leading-order monte carlo for heavy flavour hadroproduction, *J. High Energy Phys.* 09 (2007) 126, <https://doi.org/10.1088/1126-6708/2007/09/126>, arXiv:0707.3088.
- [56] S. Frixione, P. Nason, C. Oleari, Matching NLO QCD computations with Parton Shower simulations: the POWHEG method, *J. High Energy Phys.* 11 (2007) 070, <https://doi.org/10.1088/1126-6708/2007/11/070>, arXiv:0709.2092.
- [57] S. Alioli, P. Nason, C. Oleari, E. Re, A general framework for implementing NLO calculations in shower Monte Carlo programs: the POWHEG BOX, *J. High Energy Phys.* 06 (2010) 043, [https://doi.org/10.1007/JHEP06\(2010\)043](https://doi.org/10.1007/JHEP06(2010)043), arXiv:1002.2581.
- [58] S. Agostinelli, et al., GEANT4 Collaboration, GEANT4—a simulation toolkit, *Nucl. Instrum. Methods Phys. Res., Sect. A* 506 (2003) 250, [https://doi.org/10.1016/S0168-9002\(03\)01368-8](https://doi.org/10.1016/S0168-9002(03)01368-8).
- [59] J. Allison, et al., Geant4 developments and applications, *IEEE Trans. Nucl. Sci.* 53 (2006) 270, <https://doi.org/10.1109/TNS.2006.869826>.
- [60] CMS Collaboration, Measurement of the inelastic proton–proton cross section at $\sqrt{s} = 13$ TeV, arXiv:1802.02613, *J. High Energy Phys.* (2018), submitted for publication.
- [61] D. Krohn, J. Thaler, L.-T. Wang, Jet trimming, *J. High Energy Phys.* 02 (2010) 084, [https://doi.org/10.1007/JHEP02\(2010\)084](https://doi.org/10.1007/JHEP02(2010)084), arXiv:0912.1342.
- [62] D. Bertolini, P. Harris, M. Low, N. Tran, Pileup per particle identification, *J. High Energy Phys.* 10 (2014) 059, [https://doi.org/10.1007/JHEP10\(2014\)059](https://doi.org/10.1007/JHEP10(2014)059), arXiv:1407.6013.
- [63] CMS Collaboration, Jet energy scale and resolution in the CMS experiment in pp collisions at 8 TeV, *J. Instrum.* 12 (2017) P02014, <https://doi.org/10.1088/1748-0221/12/02/P02014>, arXiv:1607.03663.
- [64] CMS Collaboration, Jet Energy Scale and Resolution Performances with 13 TeV Data, CMS Detector Performance Summary CMS-DP-2016-020, CERN, 2016, <https://cds.cern.ch/record/2160347>.
- [65] CMS Collaboration, Performance of electron reconstruction and selection with the CMS detector in proton–proton collisions at $\sqrt{s} = 8$ TeV, *J. Instrum.* 10 (2015) P06005, <https://doi.org/10.1088/1748-0221/10/06/P06005>, arXiv:1502.02701.
- [66] CMS Collaboration, Performance of CMS muon reconstruction in pp collision events at $\sqrt{s} = 7$ TeV, *J. Instrum.* 7 (2012) P10002, <https://doi.org/10.1088/1748-0221/7/10/P10002>, arXiv:1206.4071.
- [67] G.P. Salam, Towards jetography, *Eur. Phys. J. C* 67 (2010) 637, <https://doi.org/10.1140/epjc/s10052-010-1314-6>, arXiv:0906.1833.
- [68] M. Dasgupta, A. Fregoso, S. Marzani, G.P. Salam, Towards an understanding of jet substructure, *J. High Energy Phys.* 09 (2013) 029, [https://doi.org/10.1007/JHEP09\(2013\)029](https://doi.org/10.1007/JHEP09(2013)029), arXiv:1307.0007.
- [69] A.J. Larkoski, S. Marzani, G. Soyez, J. Thaler, Soft drop, *J. High Energy Phys.* 05 (2014) 146, [https://doi.org/10.1007/JHEP05\(2014\)146](https://doi.org/10.1007/JHEP05(2014)146), arXiv:1402.2657.
- [70] CMS Collaboration, Jet algorithms performance in 13 TeV data, CMS Physics Analysis Summary CMS-PAS-JME-16-003, CERN, 2017, <https://cds.cern.ch/record/2256875>.
- [71] J. Thaler, K. Van Tilburg, Maximizing boosted top identification by minimizing N-subjettiness, *J. High Energy Phys.* 02 (2012) 093, [https://doi.org/10.1007/JHEP02\(2012\)093](https://doi.org/10.1007/JHEP02(2012)093), arXiv:1108.2701.
- [72] CMS Collaboration, Identification of heavy-flavour jets with the CMS detector in pp collisions at 13 TeV, arXiv:1712.07158, 2017, *J. Instrum.* (2018), submitted for publication.
- [73] ATLAS and CMS Collaborations, Combined measurement of the Higgs boson mass in pp collisions at $\sqrt{s} = 7$ and 8 tev with the ATLAS and CMS experiments, *Phys. Rev. Lett.* 114 (2015) 191803, <https://doi.org/10.1103/PhysRevLett.114.191803>, arXiv:1503.07589.
- [74] CMS Collaboration, Measurements of properties of the Higgs boson decaying into the four-lepton final state in pp collisions at $\sqrt{s} = 13$ TeV, *J. High Energy Phys.* 11 (2017) 047, [https://doi.org/10.1007/JHEP11\(2017\)047](https://doi.org/10.1007/JHEP11(2017)047), arXiv:1706.09936, 2017.
- [75] M. Oreglia, A Study of the Reactions $\psi' \rightarrow \gamma\gamma\psi$, Ph.D. thesis, SLAC, 1980, <http://www.slac.stanford.edu/pubs/slacreports/slac-r-236.html>.
- [76] F. Garwood, (i) Fiducial limits for the Poisson distribution, *Biometrika* 28 (1936) 437, <https://doi.org/10.1093/biomet/28.3-4.437>.
- [77] R.G. Lomax, D.L. Hahs-Vaughn, *Statistical Concepts: A Second Course*, Taylor and Francis, Hoboken, NJ, 2012, <https://cds.cern.ch/record/1487958>.
- [78] CMS Collaboration, CMS Luminosity Measurement for the 2016 Data Taking Period, CMS Physics Analysis Summary CMS-PAS-LUM-17-001, CERN, 2017, in preparation.
- [79] R. Barlow, C. Beeston, Fitting using finite Monte Carlo samples, *Comput. Phys. Commun.* 77 (1993) 219, [https://doi.org/10.1016/0010-4655\(93\)90005-W](https://doi.org/10.1016/0010-4655(93)90005-W).
- [80] J.S. Conway, Incorporating nuisance parameters in likelihoods for multisource spectra, in: *Proceedings, PHYSTAT 2011 Workshop on Statistical Issues Related to Discovery Claims in Search Experiments and Unfolding*, CERN, Geneva, Switzerland 17–20 January 2011, 2011, p. 115, <https://doi.org/10.5170/CERN-2011-006.115>, arXiv:1103.0354.
- [81] A.L. Read, Presentation of search results: the CL_s technique, *J. Phys. G* 28 (2002) 2693, <https://doi.org/10.1088/0954-3899/28/10/313>.
- [82] T. Junk, Confidence level computation for combining searches with small statistics, *Nucl. Instrum. Methods Phys. Res., Sect. A* 434 (1999) 435, [https://doi.org/10.1016/S0168-9002\(99\)00498-2](https://doi.org/10.1016/S0168-9002(99)00498-2), arXiv:hep-ex/9902006.
- [83] G. Cowan, K. Cranmer, E. Gross, O. Vitells, Asymptotic formulae for likelihood-based tests of new physics, *Eur. Phys. J. C* 71 (2011) 1554, <https://doi.org/10.1140/epjc/s10052-011-1554-0>, arXiv:1007.1727, Erratum: <https://doi.org/10.1140/epjc/s10052-013-2501-z>.

The CMS Collaboration

A.M. Sirunyan, A. Tumasyan

Yerevan Physics Institute, Yerevan, Armenia

W. Adam, F. Ambroggi, E. Asilar, T. Bergauer, J. Brandstetter, E. Brondolin, M. Dragicevic, J. Erö, M. Flechl, M. Friedl, R. Frühwirth¹, V.M. Ghete, J. Grossmann, J. Hrubec, M. Jeitler¹, A. König, N. Krammer, I. Krätschmer, D. Liko, T. Madlener, I. Mikulec, E. Pree, N. Rad, H. Rohringer, J. Schieck¹, R. Schöfbeck, M. Spanring, D. Spitzbart, W. Waltenberger, J. Wittmann, C.-E. Wulz¹, M. Zarucki

Institut für Hochenergiephysik, Wien, Austria

V. Chekhovsky, V. Mossolov, J. Suarez Gonzalez

Institute for Nuclear Problems, Minsk, Belarus

E.A. De Wolf, D. Di Croce, X. Janssen, J. Lauwers, M. Van De Klundert, H. Van Haevermaet, P. Van Mechelen, N. Van Remortel

Universiteit Antwerpen, Antwerpen, Belgium

S. Abu Zeid, F. Blekman, J. D'Hondt, I. De Bruyn, J. De Clercq, K. Deroover, G. Flouris, D. Lontkovskiy, S. Lowette, S. Moortgat, L. Moreels, Q. Python, K. Skovpen, S. Tavernier, W. Van Doninck, P. Van Mulders, I. Van Parijs

Vrije Universiteit Brussel, Brussel, Belgium

D. Beghin, H. Brun, B. Clerbaux, G. De Lentdecker, H. Delannoy, B. Dorney, G. Fasanella, L. Favart, R. Goldouzian, A. Grebenyuk, G. Karapostoli, T. Lenzi, J. Luetic, T. Maerschalk, A. Marinov, A. Randle-conde, T. Seva, E. Starling, C. Vander Velde, P. Vanlaer, D. Vannerom, R. Yonamine, F. Zenoni, F. Zhang²

Université Libre de Bruxelles, Bruxelles, Belgium

A. Cimmino, T. Cornelis, D. Dobur, A. Fagot, M. Gul, I. Khvastunov³, D. Poyraz, C. Roskas, S. Salva, M. Tytgat, W. Verbeke, N. Zaganidis

Ghent University, Ghent, Belgium

H. Bakhshiansohi, O. Bondu, S. Brochet, G. Bruno, C. Caputo, A. Caudron, P. David, S. De Visscher, C. Delaere, M. Delcourt, B. Francois, A. Giammanco, M. Komm, G. Krintiras, V. Lemaitre, A. Magitteri, A. Mertens, M. Musich, K. Piotrkowski, L. Quertenmont, A. Saggio, M. Vidal Marono, S. Wertz, J. Zobec

Université Catholique de Louvain, Louvain-la-Neuve, Belgium

N. Beliy

Université de Mons, Mons, Belgium

W.L. Aldá Júnior, F.L. Alves, G.A. Alves, L. Brito, M. Correa Martins Junior, C. Hensel, A. Moraes, M.E. Pol, P. Rebello Teles

Centro Brasileiro de Pesquisas Físicas, Rio de Janeiro, Brazil

E. Belchior Batista Das Chagas, W. Carvalho, J. Chinellato⁴, E. Coelho, E.M. Da Costa, G.G. Da Silveira⁵, D. De Jesus Damiao, S. Fonseca De Souza, L.M. Huertas Guativa, H. Malbouisson, M. Melo De Almeida, C. Mora Herrera, L. Mundim, H. Nogima, L.J. Sanchez Rosas, A. Santoro, A. Sznajder, M. Thiel, E.J. Tonelli Manganote⁴, F. Torres Da Silva De Araujo, A. Vilela Pereira

Universidade do Estado do Rio de Janeiro, Rio de Janeiro, Brazil

S. Ahuja^a, C.A. Bernardes^a, T.R. Fernandez Perez Tomei^a, E.M. Gregores^b, P.G. Mercadante^b, S.F. Novaes^a, Sandra S. Padula^a, D. Romero Abad^b, J.C. Ruiz Vargas^a

^a *Universidade Estadual Paulista, São Paulo, Brazil*

^b *Universidade Federal do ABC, São Paulo, Brazil*

A. Aleksandrov, R. Hadjiiska, P. Iaydjiev, M. Misheva, M. Rodozov, M. Shopova, G. Sultanov

Institute for Nuclear Research and Nuclear Energy of Bulgaria Academy of Sciences, Bulgaria

A. Dimitrov, I. Glushkov, L. Litov, B. Pavlov, P. Petkov

University of Sofia, Sofia, Bulgaria

W. Fang⁶, X. Gao⁶, L. Yuan

Beihang University, Beijing, China

M. Ahmad, J.G. Bian, G.M. Chen, H.S. Chen, M. Chen, Y. Chen, C.H. Jiang, D. Leggat, H. Liao, Z. Liu, F. Romeo, S.M. Shaheen, A. Spiezia, J. Tao, C. Wang, Z. Wang, E. Yazgan, H. Zhang, S. Zhang, J. Zhao

Institute of High Energy Physics, Beijing, China

Y. Ban, G. Chen, Q. Li, S. Liu, Y. Mao, S.J. Qian, D. Wang, Z. Xu

State Key Laboratory of Nuclear Physics and Technology, Peking University, Beijing, China

C. Avila, A. Cabrera, L.F. Chaparro Sierra, C. Florez, C.F. González Hernández, J.D. Ruiz Alvarez

Universidad de Los Andes, Bogota, Colombia

B. Courbon, N. Godinovic, D. Lelas, I. Puljak, P.M. Ribeiro Cipriano, T. Sculac

University of Split, Faculty of Electrical Engineering, Mechanical Engineering and Naval Architecture, Split, Croatia

Z. Antunovic, M. Kovac

University of Split, Faculty of Science, Split, Croatia

V. Brigljevic, D. Ferencek, K. Kadija, B. Mesic, A. Starodumov⁷, T. Susa

Institute Rudjer Boskovic, Zagreb, Croatia

M.W. Ather, A. Attikis, G. Mavromanolakis, J. Mousa, C. Nicolaou, F. Ptochos, P.A. Razis, H. Rykaczewski

University of Cyprus, Nicosia, Cyprus

M. Finger⁸, M. Finger Jr.⁸

Charles University, Prague, Czech Republic

E. Carrera Jarrin

Universidad San Francisco de Quito, Quito, Ecuador

A.A. Abdelalim^{9,10}, Y. Mohammed¹¹, E. Salama^{12,13}

Academy of Scientific Research and Technology of the Arab Republic of Egypt, Egyptian Network of High Energy Physics, Cairo, Egypt

R.K. Dewanjee, M. Kadastik, L. Perrini, M. Raidal, A. Tiko, C. Veelken

National Institute of Chemical Physics and Biophysics, Tallinn, Estonia

P. Eerola, H. Kirschenmann, J. Pekkanen, M. Voutilainen

Department of Physics, University of Helsinki, Helsinki, Finland

J. Havukainen, J.K. Heikkilä, T. Järvinen, V. Karimäki, R. Kinnunen, T. Lampén, K. Lassila-Perini, S. Laurila, S. Lehti, T. Lindén, P. Luukka, H. Siikonen, E. Tuominen, J. Tuominiemi

Helsinki Institute of Physics, Helsinki, Finland

J. Talvitie, T. Tuuva

Lappeenranta University of Technology, Lappeenranta, Finland

M. Besancon, F. Couderc, M. Dejardin, D. Denegri, J.L. Faure, F. Ferri, S. Ganjour, S. Ghosh, A. Givernaud, P. Gras, G. Hamel de Monchenault, P. Jarry, I. Kucher, C. Leloup, E. Locci, M. Machet, J. Malcles, G. Negro, J. Rander, A. Rosowsky, M.Ö. Sahin, M. Titov

IRFU, CEA, Université Paris-Saclay, Gif-sur-Yvette, France

A. Abdulsalam, C. Amendola, I. Antropov, S. Baffioni, F. Beaudette, P. Busson, L. Cadamuro, C. Charlot, R. Granier de Cassagnac, M. Jo, S. Lisniak, A. Lobanov, J. Martin Blanco, M. Nguyen, C. Ochando, G. Ortona, P. Paganini, P. Pigard, R. Salerno, J.B. Sauvan, Y. Sirois, A.G. Stahl Leitton, T. Strebler, Y. Yilmaz, A. Zabi, A. Zghiche

Laboratoire Leprince-Ringuet, Ecole polytechnique, CNRS/IN2P3, Université Paris-Saclay, Palaiseau, France

J.-L. Agram¹⁴, J. Andrea, D. Bloch, J.-M. Brom, M. Buttignol, E.C. Chabert, N. Chanon, C. Collard, E. Conte¹⁴, X. Coubez, J.-C. Fontaine¹⁴, D. Gelé, U. Goerlach, M. Jansová, A.-C. Le Bihan, N. Tonon, P. Van Hove

Université de Strasbourg, CNRS, IPHC UMR 7178, F-67000 Strasbourg, France

S. Gadrat

Centre de Calcul de l'Institut National de Physique Nucleaire et de Physique des Particules, CNRS/IN2P3, Villeurbanne, France

S. Beauceron, C. Bernet, G. Boudoul, R. Chierici, D. Contardo, P. Depasse, H. El Mamouni, J. Fay, L. Finco, S. Gascon, M. Gouzevitch, G. Grenier, B. Ille, F. Lagarde, I.B. Laktineh, M. Lethuillier, L. Mirabito, A.L. Pequegnot, S. Perries, A. Popov¹⁵, V. Sordini, M. Vander Donckt, S. Viret

Université de Lyon, Université Claude Bernard Lyon 1, CNRS-IN2P3, Institut de Physique Nucléaire de Lyon, Villeurbanne, France

T. Toriashvili¹⁶

Georgian Technical University, Tbilisi, Georgia

Z. Tsamalaidze⁸

Tbilisi State University, Tbilisi, Georgia

C. Autermann, L. Feld, M.K. Kiesel, K. Klein, M. Lipinski, M. Preuten, C. Schomakers, J. Schulz, V. Zhukov¹⁵

RWTH Aachen University, I. Physikalisches Institut, Aachen, Germany

A. Albert, E. Dietz-Laursonn, D. Duchardt, M. Endres, M. Erdmann, S. Erdweg, T. Esch, R. Fischer, A. Güth, M. Hamer, T. Hebbeker, C. Heidemann, K. Hoepfner, S. Knutzen, M. Merschmeyer, A. Meyer, P. Millet, S. Mukherjee, T. Pook, M. Radziej, H. Reithler, M. Rieger, F. Scheuch, D. Teyssier, S. Thüer

RWTH Aachen University, III. Physikalisches Institut A, Aachen, Germany

G. Flügge, B. Kargoll, T. Kress, A. Künsken, T. Müller, A. Nehr Korn, A. Nowack, C. Pistone, O. Pooth, A. Stahl¹⁷

RWTH Aachen University, III. Physikalisches Institut B, Aachen, Germany

M. Aldaya Martin, T. Arndt, C. Asawatrangkuldee, K. Beernaert, O. Behnke, U. Behrens, A. Bermúdez Martínez, A.A. Bin Anuar, K. Borras¹⁸, V. Botta, A. Campbell, P. Connor, C. Contreras-Campana, F. Costanza, C. Diez Pardos, G. Eckerlin, D. Eckstein, T. Eichhorn, E. Eren, E. Gallo¹⁹, J. Garay Garcia, A. Geiser, A. Gizhko, J.M. Grados Luyando, A. Grohsjean, P. Gunnellini, M. Guthoff, A. Harb, J. Hauk, M. Hempel²⁰, H. Jung, A. Kalogeropoulos, M. Kasemann, J. Keaveney, C. Kleinwort, I. Korol, D. Krücker, W. Lange, A. Lelek, T. Lenz, J. Leonard, K. Lipka, W. Lohmann²⁰, R. Mankel, I.-A. Melzer-Pellmann, A.B. Meyer, G. Mittag, J. Mnich, A. Mussgiller, E. Ntomari, D. Pitzl, A. Raspereza, B. Roland, M. Savitskyi, P. Saxena, R. Shevchenko, S. Spannagel, N. Stefaniuk, G.P. Van Onsem, R. Walsh, Y. Wen, K. Wichmann, C. Wissing, O. Zenaiev

Deutsches Elektronen-Synchrotron, Hamburg, Germany

R. Aggleton, S. Bein, V. Blobel, M. Centis Vignali, T. Dreyer, E. Garutti, D. Gonzalez, J. Haller, A. Hinzmann, M. Hoffmann, A. Karavdina, R. Klanner, R. Kogler, N. Kovalchuk, S. Kurz, T. Lapsien, I. Marchesini, D. Marconi, M. Meyer, M. Niedziela, D. Nowatschin, F. Pantaleo¹⁷, T. Peiffer, A. Perieanu,

C. Scharf, P. Schleper, A. Schmidt, S. Schumann, J. Schwandt, J. Sonneveld, H. Stadie, G. Steinbrück, F.M. Stober, M. Stöver, H. Tholen, D. Troendle, E. Usai, L. Vanelderen, A. Vanhoefer, B. Vormwald

University of Hamburg, Hamburg, Germany

M. Akbiyik, C. Barth, M. Baselga, S. Baur, E. Butz, R. Caspart, T. Chwalek, F. Colombo, W. De Boer, A. Dierlamm, N. Faltermann, B. Freund, R. Friese, M. Giffels, D. Haitz, M.A. Harrendorf, F. Hartmann¹⁷, S.M. Heindl, U. Husemann, F. Kassel¹⁷, S. Kudella, H. Mildner, M.U. Mozer, Th. Müller, M. Plagge, G. Quast, K. Rabbertz, M. Schröder, I. Shvetsov, G. Sieber, H.J. Simonis, R. Ulrich, S. Wayand, M. Weber, T. Weiler, S. Williamson, C. Wöhrmann, R. Wolf

Institut für Experimentelle Kernphysik, Karlsruhe, Germany

G. Anagnostou, G. Daskalakis, T. Geralis, V.A. Giakoumopoulou, A. Kyriakis, D. Loukas, I. Topsis-Giotis

Institute of Nuclear and Particle Physics (INPP), NCSR Demokritos, Aghia Paraskevi, Greece

G. Karathanasis, S. Kesisoglou, A. Panagiotou, N. Saoulidou

National and Kapodistrian University of Athens, Athens, Greece

K. Kousouris

National Technical University of Athens, Athens, Greece

I. Evangelou, C. Foudas, P. Kokkas, S. Mallios, N. Manthos, I. Papadopoulos, E. Paradas, J. Strologas, F.A. Triantis

University of Ioánnina, Ioánnina, Greece

M. Csanad, N. Filipovic, G. Pasztor, O. Surányi, G.I. Veres²¹

MTA-ELTE Lendület CMS Particle and Nuclear Physics Group, Eötvös Loránd University, Budapest, Hungary

G. Bencze, C. Hajdu, D. Horvath²², Á. Hunyadi, F. Sikler, V. Veszpremi

Wigner Research Centre for Physics, Budapest, Hungary

N. Beni, S. Czellar, J. Karancsi²³, A. Makovec, J. Molnar, Z. Szillasi

Institute of Nuclear Research ATOMKI, Debrecen, Hungary

M. Bartók²¹, P. Raics, Z.L. Trocsanyi, B. Ujvari

Institute of Physics, University of Debrecen, Debrecen, Hungary

S. Choudhury, J.R. Komaragiri

Indian Institute of Science (IISc), Bangalore, India

S. Bahinipati²⁴, S. Bhowmik, P. Mal, K. Mandal, A. Nayak²⁵, D.K. Sahoo²⁴, N. Sahoo, S.K. Swain

National Institute of Science Education and Research, Bhubaneswar, India

S. Bansal, S.B. Beri, V. Bhatnagar, R. Chawla, N. Dhingra, A.K. Kalsi, A. Kaur, M. Kaur, S. Kaur, R. Kumar, P. Kumari, A. Mehta, J.B. Singh, G. Walia

Panjab University, Chandigarh, India

Ashok Kumar, Aashaq Shah, A. Bhardwaj, S. Chauhan, B.C. Choudhary, R.B. Garg, S. Keshri, A. Kumar, S. Malhotra, M. Naimuddin, K. Ranjan, R. Sharma

University of Delhi, Delhi, India

R. Bhardwaj, R. Bhattacharya, S. Bhattacharya, U. Bhawandeep, S. Dey, S. Dutt, S. Dutta, S. Ghosh, N. Majumdar, A. Modak, K. Mondal, S. Mukhopadhyay, S. Nandan, A. Purohit, A. Roy, D. Roy, S. Roy Chowdhury, S. Sarkar, M. Sharan, S. Thakur

Saha Institute of Nuclear Physics, HBNI, Kolkata, India

P.K. Behera

Indian Institute of Technology Madras, Madras, India

R. Chudasama, D. Dutta, V. Jha, V. Kumar, A.K. Mohanty¹⁷, P.K. Netrakanti, L.M. Pant, P. Shukla, A. Topkar

Bhabha Atomic Research Centre, Mumbai, India

T. Aziz, S. Dugad, B. Mahakud, S. Mitra, G.B. Mohanty, N. Sur, B. Sutar

Tata Institute of Fundamental Research-A, Mumbai, India

S. Banerjee, S. Bhattacharya, S. Chatterjee, P. Das, M. Guchait, Sa. Jain, S. Kumar, M. Maity²⁶, G. Majumder, K. Mazumdar, T. Sarkar²⁶, N. Wickramage²⁷

Tata Institute of Fundamental Research-B, Mumbai, India

S. Chauhan, S. Dube, V. Hegde, A. Kapoor, K. Kothekar, S. Pandey, A. Rane, S. Sharma

Indian Institute of Science Education and Research (IISER), Pune, India

S. Chenarani²⁸, E. Eskandari Tadavani, S.M. Etesami²⁸, M. Khakzad, M. Mohammadi Najafabadi, M. Naseri, S. Paktinat Mehdiabadi²⁹, F. Rezaei Hosseinabadi, B. Safarzadeh³⁰, M. Zeinali

Institute for Research in Fundamental Sciences (IPM), Tehran, Iran

M. Felcini, M. Grunewald

University College Dublin, Dublin, Ireland

M. Abbrescia^{a,b}, C. Calabria^{a,b}, A. Colaleo^a, D. Creanza^{a,c}, L. Cristella^{a,b}, N. De Filippis^{a,c}, M. De Palma^{a,b}, F. Errico^{a,b}, L. Fiore^a, G. Iaselli^{a,c}, S. Lezki^{a,b}, G. Maggi^{a,c}, M. Maggi^a, G. Miniello^{a,b}, S. My^{a,b}, S. Nuzzo^{a,b}, A. Pompili^{a,b}, G. Pugliese^{a,c}, R. Radogna^a, A. Ranieri^a, G. Selvaggi^{a,b}, A. Sharma^a, L. Silvestris^{a,17}, R. Venditti^a, P. Verwilligen^a

^a INFN Sezione di Bari, Bari, Italy

^b Università di Bari, Bari, Italy

^c Politecnico di Bari, Bari, Italy

G. Abbiendi^a, C. Battilana^{a,b}, D. Bonacorsi^{a,b}, L. Borghonovi^{a,b}, S. Braibant-Giacomelli^{a,b}, R. Campanini^{a,b}, P. Capiluppi^{a,b}, A. Castro^{a,b}, F.R. Cavallo^a, S.S. Chhibra^a, G. Codispoti^{a,b}, M. Cuffiani^{a,b}, G.M. Dallavalle^a, F. Fabbri^a, A. Fanfani^{a,b}, D. Fasanella^{a,b}, P. Giacomelli^a, C. Grandi^a, L. Guiducci^{a,b}, S. Marcellini^a, G. Masetti^a, A. Montanari^a, F.L. Navarria^{a,b}, A. Perrotta^a, A.M. Rossi^{a,b}, T. Rovelli^{a,b}, G.P. Siroli^{a,b}, N. Tosi^a

^a INFN Sezione di Bologna, Bologna, Italy

^b Università di Bologna, Bologna, Italy

S. Albergo^{a,b}, S. Costa^{a,b}, A. Di Mattia^a, F. Giordano^{a,b}, R. Potenza^{a,b}, A. Tricomi^{a,b}, C. Tuve^{a,b}

^a INFN Sezione di Catania, Catania, Italy

^b Università di Catania, Catania, Italy

G. Barbagli^a, K. Chatterjee^{a,b}, V. Ciulli^{a,b}, C. Civinini^a, R. D'Alessandro^{a,b}, E. Focardi^{a,b}, P. Lenzi^{a,b}, M. Meschini^a, S. Paoletti^a, L. Russo^{a,31}, G. Sguazzoni^a, D. Strom^a, L. Viliani^{a,b,17}

^a INFN Sezione di Firenze, Firenze, Italy

^b Università di Firenze, Firenze, Italy

L. Benussi, S. Bianco, F. Fabbri, D. Piccolo, F. Primavera¹⁷

INFN Laboratori Nazionali di Frascati, Frascati, Italy

V. Calvelli^{a,b}, F. Ferro^a, E. Robutti^a, S. Tosi^{a,b}

^a *INFN Sezione di Genova, Genova, Italy*

^b *Università di Genova, Genova, Italy*

A. Benaglia^a, A. Beschi, L. Brianza^{a,b}, F. Brivio^{a,b}, V. Ciriolo^{a,b}, M.E. Dinardo^{a,b}, S. Fiorendi^{a,b}, S. Gennai^a, A. Ghezzi^{a,b}, P. Govoni^{a,b}, M. Malberti^{a,b}, S. Malvezzi^a, R.A. Manzoni^{a,b}, D. Menasce^a, L. Moroni^a, M. Paganoni^{a,b}, K. Pauwels^{a,b}, D. Pedrini^a, S. Pigazzini^{a,b,32}, S. Ragazzi^{a,b}, N. Redaelli^a, T. Tabarelli de Fatis^{a,b}

^a *INFN Sezione di Milano-Bicocca, Milano, Italy*

^b *Università di Milano-Bicocca, Milano, Italy*

S. Buontempo^a, N. Cavallo^{a,c}, S. Di Guida^{a,d,17}, F. Fabozzi^{a,c}, F. Fienga^{a,b}, A.O.M. Iorio^{a,b}, W.A. Khan^a, L. Lista^a, S. Meola^{a,d,17}, P. Paolucci^{a,17}, C. Sciacca^{a,b}, F. Thyssen^a

^a *INFN Sezione di Napoli, Napoli, Italy*

^b *Università di Napoli 'Federico II', Napoli, Italy*

^c *Università della Basilicata, Potenza, Italy*

^d *Università G. Marconi, Roma, Italy*

P. Azzi^a, N. Bacchetta^a, L. Benato^{a,b}, D. Bisello^{a,b}, A. Boletti^{a,b}, R. Carlin^{a,b}, A. Carvalho Antunes De Oliveira^{a,b}, P. Checchia^a, P. De Castro Manzano^a, T. Dorigo^a, U. Dosselli^a, F. Gasparini^{a,b}, U. Gasparini^{a,b}, A. Gozzelino^a, S. Lacaprara^a, M. Margoni^{a,b}, A.T. Meneguzzo^{a,b}, N. Pozzobon^{a,b}, P. Ronchese^{a,b}, R. Rossin^{a,b}, F. Simonetto^{a,b}, E. Torassa^a, M. Zanetti^{a,b}, P. Zotto^{a,b}, G. Zumerle^{a,b}

^a *INFN Sezione di Padova, Padova, Italy*

^b *Università di Padova, Padova, Italy*

^c *Università di Trento, Trento, Italy*

A. Braghieri^a, A. Magnani^a, P. Montagna^{a,b}, S.P. Ratti^{a,b}, V. Re^a, M. Ressegotti^{a,b}, C. Riccardi^{a,b}, P. Salvini^a, I. Vai^{a,b}, P. Vitulo^{a,b}

^a *INFN Sezione di Pavia, Pavia, Italy*

^b *Università di Pavia, Pavia, Italy*

L. Alunni Solestizi^{a,b}, M. Biasini^{a,b}, G.M. Bilei^a, C. Cecchi^{a,b}, D. Ciangottini^{a,b}, L. Fanò^{a,b}, P. Lariccia^{a,b}, R. Leonardi^{a,b}, E. Manoni^a, G. Mantovani^{a,b}, V. Mariani^{a,b}, M. Menichelli^a, A. Rossi^{a,b}, A. Santocchia^{a,b}, D. Spiga^a

^a *INFN Sezione di Perugia, Perugia, Italy*

^b *Università di Perugia, Perugia, Italy*

K. Androsov^a, P. Azzurri^{a,17}, G. Bagliesi^a, T. Boccali^a, L. Borrello, R. Castaldi^a, M.A. Ciocci^{a,b}, R. Dell'Orso^a, G. Fedi^a, L. Giannini^{a,c}, A. Giassi^a, M.T. Grippo^{a,31}, F. Ligabue^{a,c}, T. Lomtadze^a, E. Manca^{a,c}, G. Mandorli^{a,c}, L. Martini^{a,b}, A. Messineo^{a,b}, F. Palla^a, A. Rizzi^{a,b}, A. Savoy-Navarro^{a,33}, P. Spagnolo^a, R. Tenchini^a, G. Tonelli^{a,b}, A. Venturi^a, P.G. Verdini^a

^a *INFN Sezione di Pisa, Pisa, Italy*

^b *Università di Pisa, Pisa, Italy*

^c *Scuola Normale Superiore di Pisa, Pisa, Italy*

L. Barone^{a,b}, F. Cavallari^a, M. Cipriani^{a,b}, N. Daci^a, D. Del Re^{a,b,17}, E. Di Marco^{a,b}, M. Diemoz^a, S. Gelli^{a,b}, E. Longo^{a,b}, F. Margaroli^{a,b}, B. Marzocchi^{a,b}, P. Meridiani^a, G. Organtini^{a,b}, R. Paramatti^{a,b}, F. Preiato^{a,b}, S. Rahatlou^{a,b}, C. Rovelli^a, F. Santanastasio^{a,b}

^a *INFN Sezione di Roma, Roma, Italy*

^b *Sapienza Università di Roma, Roma, Italy*

N. Amapane ^{a,b}, R. Arcidiacono ^{a,c}, S. Argiro ^{a,b}, M. Arneodo ^{a,c}, N. Bartosik ^a, R. Bellan ^{a,b}, C. Biino ^a, N. Cartiglia ^a, F. Cenna ^{a,b}, M. Costa ^{a,b}, R. Covarelli ^{a,b}, A. Degano ^{a,b}, N. Demaria ^a, B. Kiani ^{a,b}, C. Mariotti ^a, S. Maselli ^a, E. Migliore ^{a,b}, V. Monaco ^{a,b}, E. Monteil ^{a,b}, M. Monteno ^a, M.M. Obertino ^{a,b}, L. Pacher ^{a,b}, N. Pastrone ^a, M. Pelliccioni ^a, G.L. Pinna Angioni ^{a,b}, F. Ravera ^{a,b}, A. Romero ^{a,b}, M. Ruspa ^{a,c}, R. Sacchi ^{a,b}, K. Shchelina ^{a,b}, V. Sola ^a, A. Solano ^{a,b}, A. Staiano ^a, P. Traczyk ^{a,b}

^a INFN Sezione di Torino, Torino, Italy

^b Università di Torino, Torino, Italy

^c Università del Piemonte Orientale, Novara, Italy

S. Belforte ^a, M. Casarsa ^a, F. Cossutti ^a, G. Della Ricca ^{a,b}, A. Zanetti ^a

^a INFN Sezione di Trieste, Trieste, Italy

^b Università di Trieste, Trieste, Italy

D.H. Kim, G.N. Kim, M.S. Kim, J. Lee, S. Lee, S.W. Lee, C.S. Moon, Y.D. Oh, S. Sekmen, D.C. Son, Y.C. Yang

Kyungpook National University, Daegu, Republic of Korea

A. Lee

Chonbuk National University, Jeonju, Republic of Korea

H. Kim, D.H. Moon, G. Oh

Chonnam National University, Institute for Universe and Elementary Particles, Kwangju, Republic of Korea

J.A. Brochero Cifuentes, J. Goh, T.J. Kim

Hanyang University, Seoul, Republic of Korea

S. Cho, S. Choi, Y. Go, D. Gyun, S. Ha, B. Hong, Y. Jo, Y. Kim, K. Lee, K.S. Lee, S. Lee, J. Lim, S.K. Park, Y. Roh

Korea University, Seoul, Republic of Korea

J. Almond, J. Kim, J.S. Kim, H. Lee, K. Lee, K. Nam, S.B. Oh, B.C. Radburn-Smith, S.h. Seo, U.K. Yang, H.D. Yoo, G.B. Yu

Seoul National University, Seoul, Republic of Korea

M. Choi, H. Kim, J.H. Kim, J.S.H. Lee, I.C. Park

University of Seoul, Seoul, Republic of Korea

Y. Choi, C. Hwang, J. Lee, I. Yu

Sungkyunkwan University, Suwon, Republic of Korea

V. Dudenas, A. Juodagalvis, J. Vaitkus

Vilnius University, Vilnius, Lithuania

I. Ahmed, Z.A. Ibrahim, M.A.B. Md Ali ³⁴, F. Mohamad Idris ³⁵, W.A.T. Wan Abdullah, M.N. Yusli, Z. Zolkapli

National Centre for Particle Physics, Universiti Malaya, Kuala Lumpur, Malaysia

R. Reyes-Almanza, G. Ramirez-Sanchez, M.C. Duran-Osuna, H. Castilla-Valdez, E. De La Cruz-Burelo, I. Heredia-De La Cruz ³⁶, R.I. Rabadan-Trejo, R. Lopez-Fernandez, J. Mejia Guisao, A. Sanchez-Hernandez

Centro de Investigacion y de Estudios Avanzados del IPN, Mexico City, Mexico

S. Carrillo Moreno, C. Oropeza Barrera, F. Vazquez Valencia

Universidad Iberoamericana, Mexico City, Mexico

I. Pedraza, H.A. Salazar Ibarguen, C. Uribe Estrada

Benemerita Universidad Autonoma de Puebla, Puebla, Mexico

A. Morelos Pineda

Universidad Autónoma de San Luis Potosí, San Luis Potosí, Mexico

D. Krofcheck

University of Auckland, Auckland, New Zealand

P.H. Butler

University of Canterbury, Christchurch, New Zealand

A. Ahmad, M. Ahmad, Q. Hassan, H.R. Hoorani, A. Saddique, M.A. Shah, M. Shoaib, M. Waqas

National Centre for Physics, Quaid-I-Azam University, Islamabad, Pakistan

H. Bialkowska, M. Bluj, B. Boimska, T. Frueboes, M. Górski, M. Kazana, K. Nawrocki, M. Szeleper, P. Zalewski

National Centre for Nuclear Research, Swierk, Poland

K. Bunkowski, A. Byszuk³⁷, K. Doroba, A. Kalinowski, M. Konecki, J. Krolikowski, M. Misiura, M. Olszewski, A. Pyskir, M. Walczak

Institute of Experimental Physics, Faculty of Physics, University of Warsaw, Warsaw, Poland

P. Bargassa, C. Beirão Da Cruz E Silva, A. Di Francesco, P. Faccioli, B. Galinhas, M. Gallinaro, J. Hollar, N. Leonardo, L. Lloret Iglesias, M.V. Nemallapudi, J. Seixas, G. Strong, O. Toldaiev, D. Vadrucchio, J. Varela

Laboratório de Instrumentação e Física Experimental de Partículas, Lisboa, Portugal

S. Afanasiev, P. Bunin, M. Gavrilenko, I. Golutvin, I. Gorbunov, A. Kamenev, V. Karjavin, A. Lanev, A. Malakhov, V. Matveev^{38,39}, V. Palichik, V. Perelygin, S. Shmatov, S. Shulha, N. Skatchkov, V. Smirnov, N. Voytishin, A. Zarubin

Joint Institute for Nuclear Research, Dubna, Russia

Y. Ivanov, V. Kim⁴⁰, E. Kuznetsova⁴¹, P. Levchenko, V. Murzin, V. Oreshkin, I. Smirnov, V. Sulimov, L. Uvarov, S. Vavilov, A. Vorobyev

Petersburg Nuclear Physics Institute, Gatchina (St. Petersburg), Russia

Yu. Andreev, A. Dermenev, S. Gninenko, N. Golubev, A. Karneyeu, M. Kirsanov, N. Krasnikov, A. Pashenkov, D. Tliso, A. Toropin

Institute for Nuclear Research, Moscow, Russia

V. Epshteyn, V. Gavrilov, N. Lychkovskaya, V. Popov, I. Pozdnyakov, G. Safronov, A. Spiridonov, A. Stepanov, M. Toms, E. Vlasov, A. Zhokin

Institute for Theoretical and Experimental Physics, Moscow, Russia

T. Aushev, A. Bylinkin³⁹

Moscow Institute of Physics and Technology, Moscow, Russia

R. Chistov⁴², M. Danilov⁴², P. Parygin, D. Philippov, S. Polikarpov, E. Tarkovskii

National Research Nuclear University 'Moscow Engineering Physics Institute' (MEPhI), Moscow, Russia

V. Andreev, M. Azarkin³⁹, I. Dremin³⁹, M. Kirakosyan³⁹, A. Terkulov

P.N. Lebedev Physical Institute, Moscow, Russia

A. Baskakov, A. Belyaev, E. Boos, V. Bunichev, M. Dubinin⁴³, L. Dudko, A. Gribushin, V. Klyukhin, O. Kodolova, I. Lokhtin, I. Miagkov, S. Obraztsov, M. Perfilov, S. Petrushanko, V. Savrin

Skobeltsyn Institute of Nuclear Physics, Lomonosov Moscow State University, Moscow, Russia

V. Blinov⁴⁴, Y. Skovpen⁴⁴, D. Shtol⁴⁴

Novosibirsk State University (NSU), Novosibirsk, Russia

I. Azhgirey, I. Bayshev, S. Bitioukov, D. Elumakhov, V. Kachanov, A. Kalinin, D. Konstantinov, P. Mandrik, V. Petrov, R. Ryutin, A. Sobol, S. Troshin, N. Tyurin, A. Uzunian, A. Volkov

State Research Center of Russian Federation, Institute for High Energy Physics, Protvino, Russia

P. Adzic⁴⁵, P. Cirkovic, D. Devetak, M. Dordevic, J. Milosevic, V. Rekovic

University of Belgrade, Faculty of Physics and Vinca Institute of Nuclear Sciences, Belgrade, Serbia

J. Alcaraz Maestre, M. Barrio Luna, M. Cerrada, N. Colino, B. De La Cruz, A. Delgado Peris, A. Escalante Del Valle, C. Fernandez Bedoya, J.P. Fernández Ramos, J. Flix, M.C. Fouz, O. Gonzalez Lopez, S. Goy Lopez, J.M. Hernandez, M.I. Josa, D. Moran, A. Pérez-Calero Yzquierdo, J. Puerta Pelayo, A. Quintario Olmeda, I. Redondo, L. Romero, M.S. Soares, A. Álvarez Fernández

Centro de Investigaciones Energéticas Medioambientales y Tecnológicas (CIEMAT), Madrid, Spain

C. Albajar, J.F. de Trocóniz, M. Missiroli

Universidad Autónoma de Madrid, Madrid, Spain

J. Cuevas, C. Erice, J. Fernandez Menendez, I. Gonzalez Caballero, J.R. González Fernández, E. Palencia Cortezon, S. Sanchez Cruz, P. Vischia, J.M. Vizan Garcia

Universidad de Oviedo, Oviedo, Spain

I.J. Cabrillo, A. Calderon, B. Chazin Quero, E. Curras, J. Duarte Campderros, M. Fernandez, J. Garcia-Ferrero, G. Gomez, A. Lopez Virto, J. Marco, C. Martinez Rivero, P. Martinez Ruiz del Arbol, F. Matorras, J. Piedra Gomez, T. Rodrigo, A. Ruiz-Jimeno, L. Scodellaro, N. Trevisani, I. Vila, R. Vilar Cortabitarte

Instituto de Física de Cantabria (IFCA), CSIC-Universidad de Cantabria, Santander, Spain

D. Abbaneo, B. Akgun, E. Auffray, P. Baillon, A.H. Ball, D. Barney, J. Bendavid, M. Bianco, P. Bloch, A. Bocci, C. Botta, T. Camporesi, R. Castello, M. Cepeda, G. Cerminara, E. Chapon, Y. Chen, D. d'Enterria, A. Dabrowski, V. Daponte, A. David, M. De Gruttola, A. De Roeck, N. Deelen, M. Dobson, T. du Pree, M. Dünser, N. Dupont, A. Elliott-Peisert, P. Everaerts, F. Fallavollita, G. Franzoni, J. Fulcher, W. Funk, D. Gigi, A. Gilbert, K. Gill, F. Glege, D. Gulhan, P. Harris, J. Hegeman, V. Innocente, A. Jafari, P. Janot, O. Karacheban²⁰, J. Kieseler, V. Knünz, A. Kornmayer, M.J. Kortelainen, M. Krammer¹, C. Lange, P. Lecoq, C. Lourenço, M.T. Lucchini, L. Malgeri, M. Mannelli, A. Martelli, F. Meijers, J.A. Merlin, S. Mersi, E. Meschi, P. Milenovic⁴⁶, F. Moortgat, M. Mulders, H. Neugebauer, J. Ngadiuba, S. Orfanelli, L. Orsini, L. Pape, E. Perez, M. Peruzzi, A. Petrilli, G. Petrucciani, A. Pfeiffer, M. Pierini, D. Rabaday, A. Racz, T. Reis, G. Rolandi⁴⁷, M. Rovere, H. Sakulin, C. Schäfer, C. Schwick, M. Seidel, M. Selvaggi, A. Sharma, P. Silva, P. Sphicas⁴⁸, A. Stakia, J. Steggemann, M. Stoye, M. Tosi, D. Treille, A. Triossi, A. Tsirou, V. Veckalns⁴⁹, M. Verweij, W.D. Zeuner

CERN, European Organization for Nuclear Research, Geneva, Switzerland

W. Bertl[†], L. Caminada⁵⁰, K. Deiters, W. Erdmann, R. Horisberger, Q. Ingram, H.C. Kaestli, D. Kotlinski, U. Langenegger, T. Rohe, S.A. Wiederkehr

Paul Scherrer Institut, Villigen, Switzerland

M. Backhaus, L. Bäni, P. Berger, L. Bianchini, B. Casal, G. Dissertori, M. Dittmar, M. Donegà, C. Dorfer, C. Grab, C. Heidegger, D. Hits, J. Hoss, G. Kasieczka, T. Klijsma, W. Lustermann, B. Mangano, M. Marionneau, M.T. Meinhard, D. Meister, F. Micheli, P. Musella, F. Nessi-Tedaldi, F. Pandolfi, J. Pata, F. Pauss, G. Perrin, L. Perrozzi, M. Quittnat, M. Reichmann, D.A. Sanz Becerra, M. Schönenberger, L. Shchutska, V.R. Tavolaro, K. Theofilatos, M.L. Vesterbacka Olsson, R. Wallny, D.H. Zhu

ETH Zurich - Institute for Particle Physics and Astrophysics (IPA), Zurich, Switzerland

T.K. Aarrestad, C. Amsler⁵¹, M.F. Canelli, A. De Cosa, R. Del Burgo, S. Donato, C. Galloni, T. Hreus, B. Kilminster, D. Pinna, G. Rauco, P. Robmann, D. Salerno, K. Schweiger, C. Seitz, Y. Takahashi, A. Zucchetta

Universität Zürich, Zurich, Switzerland

V. Candelise, C.W. Chen, G.I. De Leon, T.H. Doan, Sh. Jain, R. Khurana, C.M. Kuo, W. Lin, A. Pozdnyakov, S.S. Yu

National Central University, Chung-Li, Taiwan

Arun Kumar, P. Chang, Y. Chao, K.F. Chen, P.H. Chen, F. Fiori, W.-S. Hou, Y. Hsiung, Y.F. Liu, R.-S. Lu, E. Paganis, A. Psallidas, A. Steen, J.f. Tsai

National Taiwan University (NTU), Taipei, Taiwan

B. Asavapibhop, K. Kovitangoon, G. Singh, N. Srimanobhas

Chulalongkorn University, Faculty of Science, Department of Physics, Bangkok, Thailand

F. Boran, S. Cerci⁵², S. Damarseckin, Z.S. Demiroglu, C. Dozen, I. Dumanoglu, S. Girgis, G. Gokbulut, Y. Guler, I. Hos⁵³, E.E. Kangal⁵⁴, O. Kara, A. Kayis Topaksu, U. Kiminsu, M. Oglakci, G. Onengut⁵⁵, K. Ozdemir⁵⁶, D. Sunar Cerci⁵², B. Tali⁵², S. Turkcapar, I.S. Zorbakir, C. Zorbilmez

Çukurova University, Physics Department, Science and Art Faculty, Adana, Turkey

B. Bilin, G. Karapinar⁵⁷, K. Ocalan⁵⁸, M. Yalvac, M. Zeyrek

Middle East Technical University, Physics Department, Ankara, Turkey

E. Gülmez, M. Kaya⁵⁹, O. Kaya⁶⁰, S. Tekten, E.A. Yetkin⁶¹

Bogazici University, Istanbul, Turkey

M.N. Agaras, S. Atay, A. Cakir, K. Cankocak

Istanbul Technical University, Istanbul, Turkey

B. Grynyov

Institute for Scintillation Materials of National Academy of Science of Ukraine, Kharkov, Ukraine

L. Levchuk

National Scientific Center, Kharkov Institute of Physics and Technology, Kharkov, Ukraine

F. Ball, L. Beck, J.J. Brooke, D. Burns, E. Clement, D. Cussans, O. Davignon, H. Flacher, J. Goldstein, G.P. Heath, H.F. Heath, J. Jacob, L. Kreczko, D.M. Newbold⁶², S. Paramesvaran, T. Sakuma, S. Seif El Nasr-storey, D. Smith, V.J. Smith

University of Bristol, Bristol, United Kingdom

K.W. Bell, A. Belyaev⁶³, C. Brew, R.M. Brown, L. Calligaris, D. Cieri, D.J.A. Cockerill, J.A. Coughlan, K. Harder, S. Harper, E. Olaiya, D. Petyt, C.H. Shepherd-Themistocleous, A. Thea, I.R. Tomalin, T. Williams

Rutherford Appleton Laboratory, Didcot, United Kingdom

G. Auzinger, R. Bainbridge, J. Borg, S. Breeze, O. Buchmuller, A. Bundock, S. Casasso, M. Citron, D. Colling, L. Corpe, P. Dauncey, G. Davies, A. De Wit, M. Della Negra, R. Di Maria, A. Elwood, Y. Haddad, G. Hall, G. Iles, T. James, R. Lane, C. Laner, L. Lyons, A.-M. Magnan, S. Malik, L. Mastrolorenzo, T. Matsushita, J. Nash, A. Nikitenko⁷, V. Palladino, M. Pesaresi, D.M. Raymond, A. Richards, A. Rose, E. Scott, C. Seez, A. Shtipliyski, S. Summers, A. Tapper, K. Uchida, M. Vazquez Acosta⁶⁴, T. Virdee¹⁷, N. Wardle, D. Winterbottom, J. Wright, S.C. Zenz

Imperial College, London, United Kingdom

J.E. Cole, P.R. Hobson, A. Khan, P. Kyberd, I.D. Reid, P. Symonds, L. Teodorescu, M. Turner, S. Zahid

Brunel University, Uxbridge, United Kingdom

A. Borzou, K. Call, J. Dittmann, K. Hatakeyama, H. Liu, N. Pastika, C. Smith

Baylor University, Waco, USA

R. Bartek, A. Dominguez

Catholic University of America, Washington DC, USA

A. Buccilli, S.I. Cooper, C. Henderson, P. Rumerio, C. West

The University of Alabama, Tuscaloosa, USA

D. Arcaro, A. Avetisyan, T. Bose, D. Gastler, D. Rankin, C. Richardson, J. Rohlf, L. Sulak, D. Zou

Boston University, Boston, USA

G. Benelli, D. Cutts, A. Garabedian, M. Hadley, J. Hakala, U. Heintz, J.M. Hogan, K.H.M. Kwok, E. Laird, G. Landsberg, J. Lee, Z. Mao, M. Narain, J. Pazzini, S. Piperov, S. Sagir, R. Syarif, D. Yu

Brown University, Providence, USA

R. Band, C. Brainerd, D. Burns, M. Calderon De La Barca Sanchez, M. Chertok, J. Conway, R. Conway, P.T. Cox, R. Erbacher, C. Flores, G. Funk, M. Gardner, W. Ko, R. Lander, C. Mclean, M. Mulhearn, D. Pellett, J. Pilot, S. Shalhout, M. Shi, J. Smith, D. Stolp, K. Tos, M. Tripathi, Z. Wang

University of California, Davis, Davis, USA

M. Bachtis, C. Bravo, R. Cousins, A. Dasgupta, A. Florent, J. Hauser, M. Ignatenko, N. Mccoll, S. Regnard, D. Saltzberg, C. Schnaible, V. Valuev

University of California, Los Angeles, USA

E. Bouvier, K. Burt, R. Clare, J. Ellison, J.W. Gary, S.M.A. Ghiasi Shirazi, G. Hanson, J. Heilman, E. Kennedy, F. Lacroix, O.R. Long, M. Olmedo Negrete, M.I. Paneva, W. Si, L. Wang, H. Wei, S. Wimpenny, B.R. Yates

University of California, Riverside, Riverside, USA

J.G. Branson, S. Cittolin, M. Derdzinski, R. Gerosa, D. Gilbert, B. Hashemi, A. Holzner, D. Klein, G. Kole, V. Krutelyov, J. Letts, I. Macneill, M. Masciovecchio, D. Olivito, S. Padhi, M. Pieri, M. Sani, V. Sharma, S. Simon, M. Tadel, A. Vartak, S. Wasserbaech⁶⁵, J. Wood, F. Würthwein, A. Yagil, G. Zevi Della Porta

University of California, San Diego, La Jolla, USA

N. Amin, R. Bhandari, J. Bradmiller-Feld, C. Campagnari, A. Dishaw, V. Dutta, M. Franco Sevilla, C. George, F. Golf, L. Gouskos, J. Gran, R. Heller, J. Incandela, S.D. Mullin, A. Ovcharova, H. Qu, J. Richman, D. Stuart, I. Suarez, J. Yoo

University of California, Santa Barbara - Department of Physics, Santa Barbara, USA

D. Anderson, A. Bornheim, J.M. Lawhorn, H.B. Newman, T. Nguyen, C. Pena, M. Spiropulu, J.R. Vlimant, S. Xie, Z. Zhang, R.Y. Zhu

California Institute of Technology, Pasadena, USA

M.B. Andrews, T. Ferguson, T. Mudholkar, M. Paulini, J. Russ, M. Sun, H. Vogel, I. Vorobiev, M. Weinberg

Carnegie Mellon University, Pittsburgh, USA

J.P. Cumalat, W.T. Ford, F. Jensen, A. Johnson, M. Krohn, S. Leontsinis, T. Mulholland, K. Stenson, S.R. Wagner

University of Colorado Boulder, Boulder, USA

J. Alexander, J. Chaves, J. Chu, S. Dittmer, K. Mcdermott, N. Mirman, J.R. Patterson, D. Quach, A. Rinkevicius, A. Ryd, L. Skinnari, L. Soffi, S.M. Tan, Z. Tao, J. Thom, J. Tucker, P. Wittich, M. Zientek

Cornell University, Ithaca, USA

S. Abdullin, M. Albrow, M. Alyari, G. Apollinari, A. Apresyan, A. Apyan, S. Banerjee, L.A.T. Bauerdick, A. Beretvas, J. Berryhill, P.C. Bhat, G. Bolla[†], K. Burkett, J.N. Butler, A. Canepa, G.B. Cerati, H.W.K. Cheung, F. Chlebana, M. Cremonesi, J. Duarte, V.D. Elvira, J. Freeman, Z. Gecse, E. Gottschalk, L. Gray, D. Green, S. Grünendahl, O. Gutsche, R.M. Harris, S. Hasegawa, J. Hirschauer, Z. Hu, B. Jayatilaka, S. Jindariani, M. Johnson, U. Joshi, B. Klima, B. Kreis, S. Lammel, D. Lincoln, R. Lipton, M. Liu, T. Liu, R. Lopes De Sá, J. Lykken, K. Maeshima, N. Magini, J.M. Marraffino, D. Mason, P. McBride, P. Merkel, S. Mrenna, S. Nahn, V. O'Dell, K. Pedro, O. Prokofyev, G. Rakness, L. Ristori, B. Schneider, E. Sexton-Kennedy, A. Soha, W.J. Spalding, L. Spiegel, S. Stoynev, J. Strait, N. Strobbe, L. Taylor, S. Tkaczyk, N.V. Tran, L. Uplegger, E.W. Vaandering, C. Vernieri, M. Verzocchi, R. Vidal, M. Wang, H.A. Weber, A. Whitbeck

Fermi National Accelerator Laboratory, Batavia, USA

D. Acosta, P. Avery, P. Bortignon, D. Bourilkov, A. Brinkerhoff, A. Carnes, M. Carver, D. Curry, R.D. Field, I.K. Furic, S.V. Gleyzer, B.M. Joshi, J. Konigsberg, A. Korytov, K. Kotov, P. Ma, K. Matchev, H. Mei, G. Mitselmakher, D. Rank, K. Shi, D. Sperka, N. Terentyev, L. Thomas, J. Wang, S. Wang, J. Yelton

University of Florida, Gainesville, USA

Y.R. Joshi, S. Linn, P. Markowitz, J.L. Rodriguez

Florida International University, Miami, USA

A. Ackert, T. Adams, A. Askew, S. Hagopian, V. Hagopian, K.F. Johnson, T. Kolberg, G. Martinez, T. Perry, H. Prosper, A. Saha, A. Santra, V. Sharma, R. Yohay

Florida State University, Tallahassee, USA

M.M. Baarmand, V. Bhopatkar, S. Colafranceschi, M. Hohlmann, D. Noonan, T. Roy, F. Yumiceva

Florida Institute of Technology, Melbourne, USA

M.R. Adams, L. Apanasevich, D. Berry, R.R. Betts, R. Cavanaugh, X. Chen, O. Evdokimov, C.E. Gerber, D.A. Hangal, D.J. Hofman, K. Jung, J. Kamin, I.D. Sandoval Gonzalez, M.B. Tonjes, H. Trauger, N. Varelas, H. Wang, Z. Wu, J. Zhang

University of Illinois at Chicago (UIC), Chicago, USA

B. Bilki⁶⁶, W. Clarida, K. Dilsiz⁶⁷, S. Durgut, R.P. Gandrajula, M. Haytmyradov, V. Khristenko, J.-P. Merlo, H. Mermerkaya⁶⁸, A. Mestvirishvili, A. Moeller, J. Nachtman, H. Ogul⁶⁹, Y. Onel, F. Ozok⁷⁰, A. Penzo, C. Snyder, E. Tiras, J. Wetzel, K. Yi

The University of Iowa, Iowa City, USA

B. Blumenfeld, A. Cocoros, N. Eminizer, D. Fehling, L. Feng, A.V. Gritsan, P. Maksimovic, J. Roskes, U. Sarica, M. Swartz, M. Xiao, C. You

Johns Hopkins University, Baltimore, USA

A. Al-bataineh, P. Baringer, A. Bean, S. Boren, J. Bowen, J. Castle, S. Khalil, A. Kropivnitskaya, D. Majumder, W. Mcbrayer, M. Murray, C. Royon, S. Sanders, E. Schmitz, J.D. Tapia Takaki, Q. Wang

The University of Kansas, Lawrence, USA

A. Ivanov, K. Kaadze, Y. Maravin, A. Mohammadi, L.K. Saini, N. Skhirtladze, S. Toda

Kansas State University, Manhattan, USA

F. Rebassoo, D. Wright

Lawrence Livermore National Laboratory, Livermore, USA

C. Anelli, A. Baden, O. Baron, A. Belloni, B. Calvert, S.C. Eno, Y. Feng, C. Ferraioli, N.J. Hadley, S. Jabeen, G.Y. Jeng, R.G. Kellogg, J. Kunkle, A.C. Mignerey, F. Ricci-Tam, Y.H. Shin, A. Skuja, S.C. Tonwar

University of Maryland, College Park, USA

D. Abercrombie, B. Allen, V. Azzolini, R. Barbieri, A. Baty, R. Bi, S. Brandt, W. Busza, I.A. Cali, M. D'Alfonso, Z. Demiragli, G. Gomez Ceballos, M. Goncharov, D. Hsu, M. Hu, Y. Iiyama, G.M. Innocenti, M. Klute, D. Kovalskyi, Y.S. Lai, Y.-J. Lee, A. Levin, P.D. Luckey, B. Maier, A.C. Marini, C. McGinn, C. Mironov, S. Narayanan, X. Niu, C. Paus, C. Roland, G. Roland, J. Salfeld-Nebgen, G.S.F. Stephans, K. Tatar, D. Velicanu, J. Wang, T.W. Wang, B. Wyslouch

Massachusetts Institute of Technology, Cambridge, USA

A.C. Benvenuti, R.M. Chatterjee, A. Evans, P. Hansen, J. Hiltbrand, S. Kalafut, Y. Kubota, Z. Lesko, J. Mans, S. Nourbakhsh, N. Ruckstuhl, R. Rusack, J. Turkewitz, M.A. Wadud

University of Minnesota, Minneapolis, USA

J.G. Acosta, S. Oliveros

University of Mississippi, Oxford, USA

E. Avdeeva, K. Bloom, D.R. Claes, C. Fangmeier, R. Gonzalez Suarez, R. Kamalieddin, I. Kravchenko, J. Monroy, J.E. Siado, G.R. Snow, B. Stieger

University of Nebraska-Lincoln, Lincoln, USA

J. Dolen, A. Godshalk, C. Harrington, I. Iashvili, D. Nguyen, A. Parker, S. Rappoccio, B. Roozbahani

State University of New York at Buffalo, Buffalo, USA

G. Alverson, E. Barberis, A. Hortiangtham, A. Massironi, D.M. Morse, T. Orimoto, R. Teixeira De Lima, D. Trocino, D. Wood

Northeastern University, Boston, USA

S. Bhattacharya, O. Charaf, K.A. Hahn, N. Mucia, N. Odell, B. Pollack, M.H. Schmitt, K. Sung, M. Trovato, M. Velasco

Northwestern University, Evanston, USA

N. Dev, M. Hildreth, K. Hurtado Anampa, C. Jessop, D.J. Karmgard, N. Kellams, K. Lannon, N. Loukas, N. Marinelli, F. Meng, C. Mueller, Y. Musienko³⁸, M. Planer, A. Reinsvold, R. Ruchti, G. Smith, S. Taroni, M. Wayne, M. Wolf, A. Woodard

University of Notre Dame, Notre Dame, USA

J. Alimena, L. Antonelli, B. Bylsma, L.S. Durkin, S. Flowers, B. Francis, A. Hart, C. Hill, W. Ji, B. Liu, W. Luo, D. Puigh, B.L. Winer, H.W. Wulsin

The Ohio State University, Columbus, USA

S. Cooperstein, O. Driga, P. Elmer, J. Hardenbrook, P. Hebda, S. Higginbotham, D. Lange, J. Luo, D. Marlow, K. Mei, I. Ojalvo, J. Olsen, C. Palmer, P. Piroué, D. Stickland, C. Tully

Princeton University, Princeton, USA

S. Malik, S. Norberg

University of Puerto Rico, Mayaguez, USA

A. Barker, V.E. Barnes, S. Das, S. Folgueras, L. Gutay, M.K. Jha, M. Jones, A.W. Jung, A. Khatiwada, D.H. Miller, N. Neumeister, C.C. Peng, H. Qiu, J.F. Schulte, J. Sun, F. Wang, W. Xie

Purdue University, West Lafayette, USA

T. Cheng, N. Parashar, J. Stupak

Purdue University Northwest, Hammond, USA

A. Adair, Z. Chen, K.M. Ecklund, S. Freed, F.J.M. Geurts, M. Guilbaud, M. Kilpatrick, W. Li, B. Michlin, M. Northup, B.P. Padley, J. Roberts, J. Rorie, W. Shi, Z. Tu, J. Zabel, A. Zhang

Rice University, Houston, USA

A. Bodek, P. de Barbaro, R. Demina, Y.t. Duh, T. Ferbel, M. Galanti, A. Garcia-Bellido, J. Han, O. Hindrichs, A. Khukhunaishvili, K.H. Lo, P. Tan, M. Verzetti

University of Rochester, Rochester, USA

R. Ciesielski, K. Goulianos, C. Mesropian

The Rockefeller University, New York, USA

A. Agapitos, J.P. Chou, Y. Gershtein, T.A. Gómez Espinosa, E. Halkiadakis, M. Heindl, E. Hughes, S. Kaplan, R. Kunnawalkam Elayavalli, S. Kyriacou, A. Lath, R. Montalvo, K. Nash, M. Osherson, H. Saka, S. Salur, S. Schnetzer, D. Sheffield, S. Somalwar, R. Stone, S. Thomas, P. Thomassen, M. Walker

Rutgers, The State University of New Jersey, Piscataway, USA

A.G. Delannoy, M. Foerster, J. Heideman, G. Riley, K. Rose, S. Spanier, K. Thapa

University of Tennessee, Knoxville, USA

O. Bouhali ⁷¹, A. Castaneda Hernandez ⁷¹, A. Celik, M. Dalchenko, M. De Mattia, A. Delgado, S. Dildick, R. Eusebi, J. Gilmore, T. Huang, T. Kamon ⁷², R. Mueller, Y. Pakhotin, R. Patel, A. Perloff, L. Perniè, D. Rathjens, A. Safonov, A. Tatarinov, K.A. Ulmer

Texas A&M University, College Station, USA

N. Akchurin, J. Damgov, F. De Guio, P.R. Duderu, J. Faulkner, E. Gurpinar, S. Kunori, K. Lamichhane, S.W. Lee, T. Libeiro, T. Mengke, S. Muthumuni, T. Peltola, S. Undleeb, I. Volobouev, Z. Wang

Texas Tech University, Lubbock, USA

S. Greene, A. Gurrola, R. Janjam, W. Johns, C. Maguire, A. Melo, H. Ni, K. Padeken, P. Sheldon, S. Tuo, J. Velkovska, Q. Xu

Vanderbilt University, Nashville, USA

M.W. Arenton, P. Barria, B. Cox, R. Hirosky, M. Joyce, A. Ledovskoy, H. Li, C. Neu, T. Sinthuprasith, Y. Wang, E. Wolfe, F. Xia

University of Virginia, Charlottesville, USA

R. Harr, P.E. Karchin, N. Poudyal, J. Sturdy, P. Thapa, S. Zaleski

Wayne State University, Detroit, USA

M. Brodski, J. Buchanan, C. Caillol, S. Dasu, L. Dodd, S. Duric, B. Gomber, M. Grothe, M. Herndon, A. Hervé, U. Hussain, P. Klabbers, A. Lanaro, A. Levine, K. Long, R. Loveless, G. Polese, T. Ruggles, A. Savin, N. Smith, W.H. Smith, D. Taylor, N. Woods

University of Wisconsin - Madison, Madison, WI, USA

[†] Deceased.

¹ Also at Vienna University of Technology, Vienna, Austria.

² Also at State Key Laboratory of Nuclear Physics and Technology, Peking University, Beijing, China.

³ Also at IRFU, CEA, Université Paris-Saclay, Gif-sur-Yvette, France.

⁴ Also at Universidade Estadual de Campinas, Campinas, Brazil.

⁵ Also at Universidade Federal de Pelotas, Pelotas, Brazil.

⁶ Also at Université Libre de Bruxelles, Bruxelles, Belgium.

⁷ Also at Institute for Theoretical and Experimental Physics, Moscow, Russia.

⁸ Also at Joint Institute for Nuclear Research, Dubna, Russia.

⁹ Also at Helwan University, Cairo, Egypt.

¹⁰ Now at Zewail City of Science and Technology, Zewail, Egypt.

¹¹ Now at Fayoum University, El-Fayoum, Egypt.

¹² Also at British University in Egypt, Cairo, Egypt.

¹³ Now at Ain Shams University, Cairo, Egypt.

¹⁴ Also at Université de Haute Alsace, Mulhouse, France.

¹⁵ Also at Skobeltsyn Institute of Nuclear Physics, Lomonosov Moscow State University, Moscow, Russia.

¹⁶ Also at Tbilisi State University, Tbilisi, Georgia.

¹⁷ Also at CERN, European Organization for Nuclear Research, Geneva, Switzerland.

¹⁸ Also at RWTH Aachen University, III. Physikalisches Institut A, Aachen, Germany.

¹⁹ Also at University of Hamburg, Hamburg, Germany.

²⁰ Also at Brandenburg University of Technology, Cottbus, Germany.

²¹ Also at MTA-ELTE Lendület CMS Particle and Nuclear Physics Group, Eötvös Loránd University, Budapest, Hungary.

²² Also at Institute of Nuclear Research ATOMKI, Debrecen, Hungary.

²³ Also at Institute of Physics, University of Debrecen, Debrecen, Hungary.

²⁴ Also at Indian Institute of Technology Bhubaneswar, Bhubaneswar, India.

²⁵ Also at Institute of Physics, Bhubaneswar, India.

²⁶ Also at University of Visva-Bharati, Santiniketan, India.

²⁷ Also at University of Ruhuna, Matara, Sri Lanka.

²⁸ Also at Isfahan University of Technology, Isfahan, Iran.

²⁹ Also at Yazd University, Yazd, Iran.

³⁰ Also at Plasma Physics Research Center, Science and Research Branch, Islamic Azad University, Tehran, Iran.

³¹ Also at Università degli Studi di Siena, Siena, Italy.

³² Also at INFN Sezione di Milano-Bicocca; Università di Milano-Bicocca, Milano, Italy.

³³ Also at Purdue University, West Lafayette, USA.

³⁴ Also at International Islamic University of Malaysia, Kuala Lumpur, Malaysia.

³⁵ Also at Malaysian Nuclear Agency, MOSTI, Kajang, Malaysia.

³⁶ Also at Consejo Nacional de Ciencia y Tecnología, Mexico city, Mexico.

³⁷ Also at Warsaw University of Technology, Institute of Electronic Systems, Warsaw, Poland.

³⁸ Also at Institute for Nuclear Research, Moscow, Russia.

³⁹ Now at National Research Nuclear University 'Moscow Engineering Physics Institute' (MEPhI), Moscow, Russia.

⁴⁰ Also at St. Petersburg State Polytechnical University, St. Petersburg, Russia.

⁴¹ Also at University of Florida, Gainesville, USA.

⁴² Also at P.N. Lebedev Physical Institute, Moscow, Russia.

⁴³ Also at California Institute of Technology, Pasadena, USA.

⁴⁴ Also at Budker Institute of Nuclear Physics, Novosibirsk, Russia.

⁴⁵ Also at Faculty of Physics, University of Belgrade, Belgrade, Serbia.

⁴⁶ Also at University of Belgrade, Faculty of Physics and Vinca Institute of Nuclear Sciences, Belgrade, Serbia.

⁴⁷ Also at Scuola Normale e Sezione dell'INFN, Pisa, Italy.

⁴⁸ Also at National and Kapodistrian University of Athens, Athens, Greece.

⁴⁹ Also at Riga Technical University, Riga, Latvia.

⁵⁰ Also at Universität Zürich, Zurich, Switzerland.

⁵¹ Also at Stefan Meyer Institute for Subatomic Physics (SMI), Vienna, Austria.

⁵² Also at Adiyaman University, Adiyaman, Turkey.

- 53 Also at Istanbul Aydin University, Istanbul, Turkey.
- 54 Also at Mersin University, Mersin, Turkey.
- 55 Also at Cag University, Mersin, Turkey.
- 56 Also at Piri Reis University, Istanbul, Turkey.
- 57 Also at Izmir Institute of Technology, Izmir, Turkey.
- 58 Also at Necmettin Erbakan University, Konya, Turkey.
- 59 Also at Marmara University, Istanbul, Turkey.
- 60 Also at Kafkas University, Kars, Turkey.
- 61 Also at Istanbul Bilgi University, Istanbul, Turkey.
- 62 Also at Rutherford Appleton Laboratory, Didcot, United Kingdom.
- 63 Also at School of Physics and Astronomy, University of Southampton, Southampton, United Kingdom.
- 64 Also at Instituto de Astrofísica de Canarias, La Laguna, Spain.
- 65 Also at Utah Valley University, Orem, USA.
- 66 Also at Beykent University, Istanbul, Turkey.
- 67 Also at Bingol University, Bingol, Turkey.
- 68 Also at Erzincan University, Erzincan, Turkey.
- 69 Also at Sinop University, Sinop, Turkey.
- 70 Also at Mimar Sinan University, Istanbul, Istanbul, Turkey.
- 71 Also at Texas A&M University at Qatar, Doha, Qatar.
- 72 Also at Kyungpook National University, Daegu, Korea.